A new solid-beam approach based on first or higher-order beam theories for finite element analysis of thin to thick structures

Guoqiang Wei, Pascal Lardeur, Frédéric Druesne

Version of Record: https://www.sciencedirect.com/science/article/pii/S0168874X21001360
Manuscript_2b0d38e78f9cddbd1e0040123f5b6962

A new solid-beam approach based on first or higher-order beam theories for finite element analysis of thin to thick structures

Guoqiang WEI, Pascal LARDEUR, Frédéric DRUESNE

Université de technologie de Compiègne, CNRS, Roberval, Mechanics energy and electricity, Centre de recherche Royallieu - CS 60 319 - 60 203 Compiègne Cedex, France

E-mail: guoqiang.wei@utc.fr

Abstract

A new solid-beam approach devoted to thin to very thick beam-like structures is proposed. To meet the beam displacement fields, kinematic relations are directly applied on the solid finite element model which contains several elements through the thickness and width. It is possible to use any beam theory based on kinematic assumptions and three theories are considered in this paper. The classical first-order beam theory, the modified first-order beam theory and a higher-order beam theory lead to the FOSB, the MFOSB and the HOSB models respectively. Linear equations due to kinematic relations are imposed at slave nodes to meet displacement fields throughout the cross-section, resulting in a reduction of the model size. Two examples are presented: a straight beam and a curved beam under distributed loading. The FOSB model gives unsatisfactory results. For a thin beam, the MFOSB model is adequate but leads to moderate errors in the thick case. Compared to the solid model, the HOSB model offers excellent displacements and stresses in thin and thick cases. The final size of these solid-beam models is slightly larger than that of an approach with classical beam elements.

Key words: Solid-beam approach; Finite element; Beam theories; Displacement field

1 Introduction

A lot of natural or industrial structures have two dimensions small compared to the third one. These structures are called beams. The first beam theory was developed during the 18th century and is known as the Euler-Bernoulli beam theory. The main assumption is that plane cross-sections normal to the undeformed neutral axis remain plane and normal to the deformed neutral axis. This theory, which does not consider transverse shear effects, is dedicated to thin beams. At the beginning of the 20th century, Timoshenko [1, 2] proposed a more general beam theory which considers transverse shear effects as well as rotatory inertia. Sections normal to the undeformed neutral axis remain plane but not necessarily normal to the deformed neutral axis. This theory can be applied to thin and thick beams. The main shortcoming of this theory is that the displacement field leads to a constant transverse shear distribution throughout the cross-section, whereas it is rather quadratic. Timoshenko introduced the so-called transverse shear correction coefficient. Then a lot of research works concerned correction coefficients. Several papers have been specifically dedicated to this issue (Cowper [3], Jensen [4] and Hutchinson [5]).

Many higher-order beam theories were developed to better describe the deformation of beams. In 1975, Essenburg [6] enriched the displacement field with a quadratic transverse displacement assumption, leading to a theory which considers transverse shear and normal strain effects. Stephen and Levinson [7] proposed a second-order beam theory which considers transverse shear stresses, transverse direct stresses and rotatory inertia. It contains two coefficients depending on the cross-section shape. Levinson [8] proposed a higher-order beam theory for rectangular cross-sections. The assumption that cross-sections normal to the undeformed neutral axis remain plane after deformation is abandoned. Indeed, a cubic distribution of axial displacement allows warping of the cross-sections. In this theory no shear coefficient is necessary. Rehfield and Murthy [9] proposed a refined beam theory accounting for transverse shear and normal effects. In its initial version, the displacement field is order 5 for the axial displacement and order 4 for the transverse displacement. Rehfield and Murthy show that an axial displacement with order 3 and a transverse displacement of order 2 is quite satisfactory and gives results very close to the exact 3D elasticity solutions. Extension to beams in space requires the consideration of other effects. Bending in the second plane can be treated like bending in the first plane. However, torsion justifies specific developments. Initially de Saint-Venant studied this phenomenon leading to the Saint-Venant's uniform torsion theory [10]. Vlasov [11] introduced the non-uniform warping deformation and this theory is suitable for thin-walled open cross-sections. Benscoter [12] proposed a more general theory which is valid for thin-walled open and also for closed cross-sections. Other 3D beam approaches require cross-section analysis to determine sectional modes to enrich the displacement fields. The so-called Generalized Beam Theory (GBT), proposed by Schardt [13] and namely developed by Habtemariam et al. [14], exploits predetermined cross-sectional deformation modes for the description of warping. The identification of these modes may be obtained by a 2D finite element analysis of the cross-section (El Fatmi [15], Naccache et El Fatmi [16]). In this approach, modes are extracted from the computation of the so-called 3D Saint-Venant's problem. Solving the Saint-Venant problem led to other beam theories (Ladevèze and Simmonds [17], Romano et al. [18], Faghidian [19]). Complementary information about beam theories can be found in the book of Goodier and Timoshenko [20]. Carrera et al. [21] proposed the Carrera Unified Formulation (CUF) which allows the use of any order polynomials to define a displacement field. Other variants of beam theories were proposed, in particular for multilayered composite structures and sandwich ones. The scope of this paper is limited to homogeneous structures, so multilayered composite structures which have led to a lot of research are not considered in this bibliography study.

The analytical resolution of examples treated with these theories is limited to some academic examples. Consequently, finite element method is widely used for the treatment of beam applications. For these finite elements, the most popular approach requires a discretization of the mid-axis and the degrees of freedom are displacements and rotations at nodes. A lot of formulations have been developed and assessed, to improve the performances of beam finite elements. Most of the formulations concern the Euler-Bernoulli and Timoshenko first-order beam theories. Finite elements based on Timoshenko theory or higher-order theories lead to several numerical problems. The most problematic one is locking, in particular transverse shear

locking, which leads to very bad results when the structure is thin. Another numerical problem, linked to the techniques used for solving the locking phenomenon, is rank deficiency which may cause spurious zero-energy modes. Several techniques were proposed to alleviate these problems. The same numerical problems exist in plate and shell finite elements and many research works were developed for this type of elements. For further information, the reader can refer to the review paper of Cen and Shang [22] which describes the state of the art concerning Reissner-Mindlin plate elements. The methods and techniques proposed to improve plate and shell elements have also been tested and adapted for beam elements. The most popular ones are reduced or selective numerical integration (Bouclier el al. [23], Adam et al. [24]), assumed natural strain (ANS) method and its variants (Bouclier el al. [23]), mixed approach (Addessi et al. [25]). Advanced beam finite elements have also been developed. Wackerfuß and Gruttmann presented the mixed hybrid beam elements based on the Hu-Washizu three-field formulation for linear and nonlinear analysis [26, 27]. This approach allows 3D constitutive laws and complete 3D stress field. Appropriate warping functions are proposed for arbitrary cross-sections. Recently Lezgy-Nazargah et al. [28] presented a quasi-3D beam finite element. The 3D beam analysis of thin-walled beams is converted into separated 2D cross-sectional for the approximation of the warping function and 1D modeling for the axial variations. The beam finite element contains three nodes and twenty-six degrees of freedom.

Several developments commented hereafter are based on a continuum theory approach but lead to beam elements which finally contain displacements and rotations, that is to say classical beam degrees of freedom. Their geometry is defined by the mid-axis, just like a classical beam element. In some cases, additional degrees of freedom are considered for representing warping of the cross-section. Lee and Kim [29] proposed the discretization of the cross-section of a beam to consider a refined warping effect. Degrees of freedom are displacements and translations, as well as numerous additional degrees of freedom for warping. Zivkovic [30] developed a beam superelement which contains 3D continuum theory for the description of the deformation of the cross-section. Curiel Sosa et al. [31] developed a continuum-based beam element which is an extension of a formulation proposed by Belytschko et al. [32], in the framework of explicit-FEM. This element uses the concept of master and slave nodes to impose beam theory kinematic assumptions. Yoon et al. [33, 34] proposed a continuum-based element built from an assemblage of solid elements. Again, beam theory assumptions are applied at cross-sectional nodes.

Another possibility is to exploit only the solid geometry, in this case a mid-axis geometry is not required, leading to the so-called solid-beam element. This approach has several advantages. First solid and solid-beam elements can be used in the same model, without difficulty. On the contrary, using classical beam and solid elements in the same model requires the development of specific solid-to-beam techniques to correctly connect beam and solid elements (Ziyaeifar and Noguchi [35]). A second advantage is that there is no need to make and exploit a mid-axis mesh, which may lead to severe difficulties and some errors for complex applications. Moreover, in the solid-beam approach, all terms of the strain and stress tensors can be considered and a three-dimensional constitutive law can be used, even if this issue may lead to

some difficulties known as the thickness locking phenomenon mentioned in this paper. Finally loading can be naturally applied on the top or bottom faces of the structure. On the contrary of elements described above, a solid-beam element looks like a solid element from a geometry point of view. Moreover, degrees of freedom are only displacements. Inspired by solid-shell elements, Frischkorn and Reese [36], who introduced the "solid-beam" expression in 2013, proposed an eight-node solid-beam element with only displacement degrees of freedom. The formulation is derived from the solid-shell formulation of Schwarze and Reese [37]. To prevent locking problems, assumed natural strain and enhanced assumed strain methods embedded in a reduced integration technique, are applied. For several linear or nonlinear examples, good results are obtained by using only one element within the cross-section. Frischkorn and Reese [38] applied this solid-beam element for the analysis of Nitinol stents. For these applications, using more than one element within the cross-section is necessary to obtain comparable results with respect to the solid solution.

In this paper, a new solid-beam approach which leads to the two advantages described above thanks to the use of solid geometry, is presented. It is based on applications of first-order or higher-order beam equations to standard solid finite element models. Our approach aims to reduce the number of degrees of freedom of the solid mesh by imposing displacement fields of beam theories. Four main original contributions can be highlighted. Firstly, one of the characteristics of our approach is that any displacement field related to various beam theories can be considered. Secondly, as a consequence of the first point, the solid-beam approach may give results very close to the reference results given by the 3D elasticity theory. Indeed, all mechanical effects of 3D elasticity theory, in particular the Poisson effect, are considered. Thirdly up to now only a limited number of research works about the solid-beam concept has been published in the literature. The fourth original point is that our solid-beam approach allows the development of a mixed model. In this case, some parts of the structure use the solid-beam approach and other parts the full solid model. This is possible without any modification of our methodology and without any particular difficulty. The paper is organized as follows. In Section 2, the basic ideas of the methodology proposed, as well as the first-order and higher-order theories of interest, are recalled. In Section 3, the approach relying on master and slave nodes concept is described. In Section 4, two examples, namely a straight beam and a curved beam, in the thin and thick cases, are treated. Moreover, a comparison with solid or beam models in terms of model size is presented. Some conclusions and perspectives are drawn in Section 5.

2 Presentation of a new solid-beam approach – theoretical aspects

2.1 Basic ideas

The new solid-beam approach is developed in the context of a general adaptive modeling methodology using solid elements only, for any type of structure. As stated above, it is often justified to apply solid theory in some areas affected by local effects, but beam or shell theory is suitable on the rest of the structure. The use of different types of elements in the same model leads to meshing difficulties and mechanical incompatibilities of the displacement field at the interfaces between beam, shell and solid areas. Namely, beam and shell elements contain

displacements and rotations but solid elements contain only displacements. Specific numerical treatment is necessary at the interfaces to improve compatibility between the different meshing areas. This approach involves theoretical problems in all cases as well as practical difficulties for complex structures. Our adaptive modeling method uses only solid elements and the mesh systematically contains several elements within the cross-section of the structure. This leads to homogeneous and regular meshes over the whole structure. There is no specific treatment in solid areas, and beam or shell displacement fields are applied in the solid-beam or solid-shell areas respectively, by using a specific approach.

In this paper, the formulation associated with the solid-beam areas is presented and assessed. Classically, to develop beam finite element models, first equations of the 3D theory of elasticity are modified to give new beam theory equations. Then, based on these equations, a beam finite element is developed, leading to a 1D mesh. The contrary is proposed here. The structure is first modeled with solid finite elements, then equations throughout the cross-section are applied directly on the solid model to modify the system of algebraic equations and obtain the beam numerical solution. The main characteristics of the new solid-beam approach are described below.

- The solid-beam model must give results very close to the reference results given by the solid model.
- First-order and higher-order beam displacement fields are considered.
- Only solid elements without severe locking phenomena are used. Our approach does not require the development of a specific solid element. In this paper, an existing hexahedral element with twenty nodes is exploited. Due to its good performances for structures submitted to bending phenomena, the C3D20 element of Abaqus has been selected for this study. Moreover, it is possible to consider a new solid element formulation.
- The formulation of the solid element is not modified and all degrees of freedom are kept at the element level. Displacements fields are directly applied at nodes of the solid finite element model after assembly. This model contains several elements through the thickness and width of the cross-section.
- The 3D constitutive law is used. It means all stresses and strains are considered in the strain energy. There is no modification of this constitutive law, consequently no use of transverse shear correction coefficients classically associated with first-order beam theories.
- From a numerical point of view, kinematic relations between the degrees of freedom of nodes throughout the cross-section, are applied. These degrees of freedom are displacements exclusively because solid elements are used. For this purpose, slave and master nodes are introduced and only master nodes are kept in the model after the application of equations. The number of master nodes in each cross-section varies depending on the chosen beam theory. This point is detailed in section 2.3.
- This process leads to a reduction of the model size and consequently of the computational cost, compared to a reference solid model.
- The refinement of mesh throughout the cross-section does not increase the final model size of our solid-beam approach.

– At the moment, only linear problems are considered. The principle of the approach is compatible with finite strains or non-linear material behavior. For the geometrical nonlinear case, kinematic equations will have to be adapted. This issue will require further works.

2.2 Displacement fields

One of the characteristics of our approach is that any displacement field related to various beam theories can be considered. In this paper three displacement fields are exploited. Existing displacement fields are reinterpreted in the context of our solid-beam approach. In particular, all the mechanical effects, namely the Poisson effect, must be taken into account to correctly describe the deformation of the cross-sections.

2.2.1 Classical first-order displacement field

The first displacement field is given by the classical Timoshenko beam theory. It considers membrane and bending effects as well as transverse shear ones. It is widely used in beam finite element formulations. This 2D displacement field is defined by:

$$\begin{cases} u(y,z) = u_0 + z\varphi_y \\ v(y,z) = 0 \\ w(y,z) = w_0 \end{cases} \quad (1)$$

where u_0 and w_0 are the displacements of a node on the mid-axis, φ_y is the rotation around y axis.

This displacement field uses displacements as well as rotations. In our approach, only displacements at nodes are used. It is relevant and well suited to rewrite the displacement field of Eq. (1) in the simple following form:

$$\begin{cases} u(y,z) = za_1 + a_2 \\ v(y,z) = 0 \\ w(y,z) = c_1 \end{cases} \quad (2)$$

where a_1, a_2 and c_1 are coefficients to be determined.

As will be shown and justified in Section 4.1.3, this displacement field does not lead to good results, in the context of our approach.

2.2.2 Modified first-order displacement field

The displacements within the cross-section of a moderately thin beam modeled with solid elements have been observed. For the bending case, the displacements *u* is linear, which fits well with the classical first-order theory. The displacement *w* is almost constant with *z* but with a slight quadratic contribution, while the classical first-order beam theory considers it as constant through the thickness. For the membrane case, the displacements *u* fits well with the classical first-order theory, showing a constant distribution. But the displacement component *w* is linear, which is different from the zero through-the-thickness assumption of the classical first-order beam theory. In summary, the classical first-order beam theory should be modified to be

completely consistent with solid theory. The displacement *w* is required to be enriched so linear and quadratic terms are added. This does not mean that the classical first-order beam theory is inconsistent. Indeed, the assumption of constant displacement *w* in this theory has no consequence on the results due to the fact that the effect of the transverse strain ε_{zz} and the transverse stress σ_{zz} are neglected. One may say that the classical first-order beam theory is self-consistent but cannot reproduce all the effects of the 3D theory of elasticity.

The consistency between linear distribution for *u* and quadratic distribution for *w* can be demonstrated. First, for a given cross-section, considering both membrane and bending effects in plane *x*-*z*, linear through-the-thickness distributions is assumed for *u*:

$$u(y,z) = za_1 + a_2 \tag{3}$$

in which a_1 and a_2 are coefficients to be determined for each cross-section. So the ε_{xx} strain is linear with respect to *z*:

$$\varepsilon_{xx} = u_{,x} = za_3 + a_4 \tag{4}$$

where a_3 and a_4 are coefficients to be determined for each cross-section.

For isotropic material, the 3D solid stress-strain relationship is:

$$\begin{Bmatrix} \varepsilon_{xx} \\ \varepsilon_{yy} \\ \varepsilon_{zz} \\ \gamma_{xy} \\ \gamma_{xz} \\ \gamma_{yz} \end{Bmatrix} = \frac{1}{E} \begin{bmatrix} 1 & -\nu & -\nu & 0 & 0 & 0 \\ -\nu & 1 & -\nu & 0 & 0 & 0 \\ -\nu & -\nu & 1 & 0 & 0 & 0 \\ 0 & 0 & 0 & 2(1+\nu) & 0 & 0 \\ 0 & 0 & 0 & 0 & 2(1+\nu) & 0 \\ 0 & 0 & 0 & 0 & 0 & 2(1+\nu) \end{bmatrix} \begin{Bmatrix} \sigma_{xx} \\ \sigma_{yy} \\ \sigma_{zz} \\ \sigma_{xy} \\ \sigma_{xz} \\ \sigma_{yz} \end{Bmatrix} \tag{5}$$

For 2D beam structures, the σ_{yy} and σ_{zz} stresses are small and can be neglected, leading to the following relations:

$$\sigma_{xx} = E\varepsilon_{xx} \tag{6}$$

$$\varepsilon_{yy} = v_{,y} = -\frac{\nu}{E}\sigma_{xx} = -\nu\varepsilon_{xx} \tag{7}$$

$$\varepsilon_{zz} = w_{,z} = -\frac{\nu}{E}\sigma_{xx} = -\nu\varepsilon_{xx} \tag{8}$$

Eqs. (7) and (8) show that ε_{yy} and ε_{zz} are due to the Poisson effect and because ε_{xx} is linear with respect to *z*, ε_{yy} and ε_{zz} must also be linear through the thickness. By integration of Eq. (7), one highlights the expression of *v*:

$$v(y,z) = yzb_1 + yb_2 + b_3 + f_1(z) \tag{9}$$

where b_1 to b_3 are coefficients and $f_1(z)$ a function to be determined for each cross-section. The coefficient b_3 represents a global displacement of a cross-section in the *y* direction. This displacement is zero for a beam in a plane, so hereafter $b_3 = 0$ is considered.

In the same way, by integration of Eq. (8), one highlights the expression of *w*:

$$w(y,z) = z^2 c_1 + z c_2 + c_3 + f_2(y) \tag{10}$$

where c_1 to c_3 are coefficients and $f_2(y)$ a function to be determined for each cross-section.

Taking into account the expressions of *v* and *w* given in Eqs. (9) and (10), the γ_{yz} strain is defined by:

$$\gamma_{yz} = v_{,z} + w_{,y} \tag{11}$$

with

$$v_{,z} = y b_1 + f_1(z)_{,z} \tag{12}$$

and

$$w_{,y} = f_2(y)_{,y} \tag{13}$$

So the γ_{yz} strain is at least linear with respect to *y* and at least constant in the *z* direction. In order to have consistent contributions of the two terms $v_{,z}$ and $w_{,y}$, they must both have a linear variation in the *y* direction. The choice to meet this condition is such that $f_1(z) = 0$ and $f_2(\mathrm{y})$ is quadratic with respect to *y*.

Finally, the modified first-order displacement field is:

$$\begin{cases} u(y,z) = z a_1 + a_2 \\ v(y,z) = yz b_1 + y b_2 \\ w(y,z) = z^2 c_1 + y^2 c_4 + z c_2 + c_3 \end{cases} \tag{14}$$

where a_1 to a_2, b_1 to b_2, c_1 to c_4 are coefficients to be determined.

To verify the relevancy of this displacement field, the deformation of the cross-section of a beam under bending or membrane loading, studied with a solid model, has been observed (see Fig. 1). The displacement field given in Eq. (14) is consistent with the results observed. In particular, in the bending case, the quadratic contribution of *w* with respect to *y* is highlighted. This displacement field allows the warping of each cross-section. Hutchinson [5] proposed a similar displacement field without consideration of the membrane effect. This displacement field can also be described by the CUF [21].

In our approach, all mechanical effects of 3D elasticity are considered. In particular, the Poisson effect is considered, this is the reason why the *v* component is bilinear and *w* is quadratic. In summary displacement field defined in Eq. (14) is consistent with 3D elasticity theory. This allows to reproduce the deformation of the cross-section as highlighted in Fig. 1. On the contrary, in the 2D beam theory, *v* and *w* are zero and constant respectively. Displacement field defined in Eq. (1) is consistent with 2D beam theory but not with 3D elasticity theory.

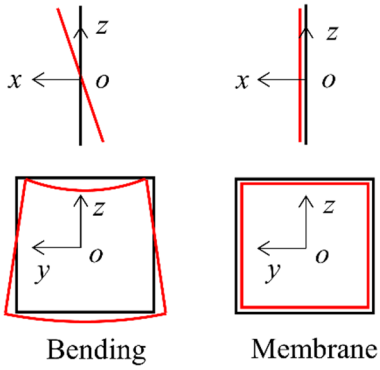

Fig. 1. Beam under bending or membrane loading – Deformation of a cross-section.

2.2.3 Higher-order displacement field

The example mentioned above is now considered for a thick beam (l/h=5). The through-the-thickness distribution of displacements is presented in Fig. 2.

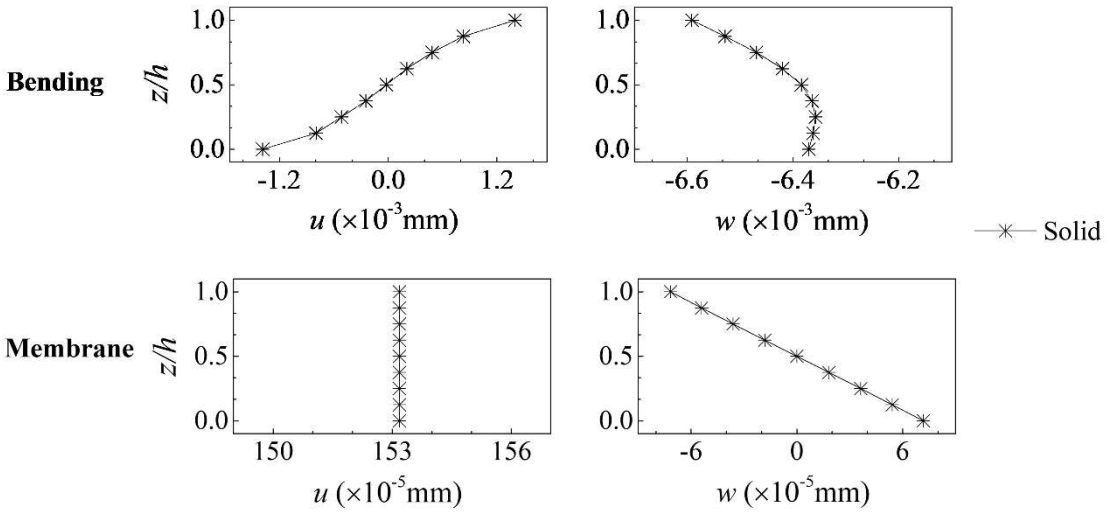

Fig. 2. Thick beam under bending or membrane loading – Distribution of through-the-thickness displacements.

For the thick beam bending case, the displacements u seems to have a cubic variation, while displacement w is again almost quadratic. The cubic distribution corresponds to the displacement u introduced by Levinson [8].

$$u(y,z) = z^3\phi_x + z\psi_x \tag{15}$$

where ϕ_x is the warping function and ψ_x represents the rotation of a cross-section of the beam.

This cubic distribution is consistent with results presented in Fig. 2. Moreover, it is a relevant choice to obtain a good approximation of transverse shear stresses through the thickness. Indeed, for a 2D beam, the distribution of σ_{xz} transverse shear stress is almost quadratic. This σ_{xz} stress is given by:

$$\sigma_{xz} = G\left(u_{,z} + w_{,x}\right) \tag{16}$$

First-order beam theories which use linear variation of *u* and constant variation of *w* through the thickness are not able to reproduce correctly transverse shear effects. Namely these assumptions lead to a constant distribution of σ_{xz} through the thickness, which is not correct. This is the reason why, from the one hand generally integration of equilibrium equations is used for calculating transverse shear stresses, and from the other hand transverse shear correction coefficient is required for the assessment of transverse shear stiffness [3, 4, 5, 6]. If *u* is cubic and *w* is quadratic with respect to *z*, both terms $u_{,z}$ and $w_{,x}$ can be quadratic with respect to *z*, leading to a consistent and precise distribution of the σ_{xz} stress, without any correction. This point is highlighted in the examples section.

Refined beam theories, namely that proposed by Levinson [8], uses the classical variables ψ_x but also another variable ϕ_x which is difficult to be interpreted and managed, for instance to define loading and boundary conditions. In the approach proposed, this difficulty is prevented because, as highlighted in Section 3, only displacements at nodes are exploited, without any other variable. For bending case, the component *u* is directly inspired by the Levinson displacement field. For the general case with membrane and bending effects a constant contribution is added for *u* while *v* and *w* are the same as for the modified first-order theory. The displacement field of the proposed refined beam theory, involving nine terms, is written as:

$$\begin{cases} u(y,z) = z^3 a_1 + z a_2 + a_3 \\ v(y,z) = yz b_1 + y b_2 \\ w(y,z) = z^2 c_1 + y^2 c_4 + z c_2 + c_3 \end{cases} \tag{17}$$

where a_1 to a_3, b_1 to b_2, c_1 to c_4 are coefficients to be determined.

This displacement field allows the warping of each cross-section. Anyway, the cubic variation of *u* had already been proposed, namely by Levinson. The displacement field as given in Eq. (17) should lead to the same global displacement compared with the Levinson theory. The difference is that our displacement field allows a detailed description of the deformation of the cross-sections, namely the Poisson effect is considered. This displacement field can also be described by the CUF [21].

3 Presentation of a new solid-beam approach – numerical aspects and implementation

This section explains how the displacement fields presented in Section 2.2 are applied on the solid element mesh, leading to solid-beam models. Equations are applied on the assembled finite element models. Three solid-beam models are described. Eq. (2) gives the First-Order Solid-Beam (FOSB) model. In the same way, Eq. (14) leads to the Modified First-Order Solid-Beam (MFOSB) model and Eq. (17) leads to the Higher-Order Solid-Beam (HOSB) one. The principle consisting of imposing a displacement field at nodes throughout the cross-section is

illustrated in Fig. 4. Master degrees of freedom and slave degrees of freedom are defined for each cross-section. All slave degrees of freedom can be eliminated from the system of equations to be solved. As highlighted in the following sections, all the relations between master and slave degrees of freedom are linear. For implementation, the "*EQUATION" keyword in Abaqus [39] is used to introduce these linear equations. In the post-processing step, displacements are available for all the nodes.

3.1 FOSB model

For each cross-section of the beam, the FOSB model uses two master nodes at points *A* and *B* as described in Fig. 3. Eq. (2) contains two coefficients a_1 and a_2 to be determined for u and one coefficient c_1 for w. To identify these three coefficients, the following set of three equations is used:

$$\begin{cases} u(y_A, z_A) = u_A = z_A a_1 + a_2 \\ u(y_B, z_B) = u_B = z_B a_1 + a_2 \\ w(y_A, z_A) = w_A = c_1 \end{cases} \tag{18}$$

where u_A, u_B, w_A are the displacements at points *A* and *B*, y_A, z_A, y_B, z_B are the coordinates of points *A* and *B* in the y and z directions.

Solving Eq. (18) gives the expressions of coefficients identified for each cross-section:

$$\begin{cases} a_1 = \dfrac{u_A - u_B}{z_A - z_B} \\ a_2 = -\dfrac{z_A u_B - z_B u_A}{z_A - z_B} \\ c_1 = w_A \end{cases} \tag{19}$$

By taking into account Eq. (19) into Eq. (2), one obtains:

$$\begin{cases} u(y, z) = z\dfrac{u_A - u_B}{z_A - z_B} + \dfrac{z_B u_A - z_A u_B}{z_A - z_B} \\ v(y, z) = 0 \\ w(y, z) = w_A \end{cases} \tag{20}$$

Linear equations to be applied are obtained by replacing z by z_i in Eq. (20), z_i being the coordinate of the slave node *i* in the z direction:

$$\begin{cases} u(y_i, z_i) = u_i^S = z_i\dfrac{u_A - u_B}{z_A - z_B} + \dfrac{z_B u_A - z_A u_B}{z_A - z_B} \\ v(y_i, z_i) = v_i^S = 0 \\ w(y_i, z_i) = w_i^S = w_A \end{cases} \tag{21}$$

For a given cross-section of the beam, the displacements u_A, u_B and w_A must be calculated because they are the master degrees of freedom. All other degrees of freedom are the slave degrees of freedom. As highlighted in Eq. (21), they can be expressed in terms of master degrees of freedom, so they can be eliminated from the system of equations to be solved. Concerning

the displacements u, Eq. (21) is applied at all nodes of the cross-sections, except points A and B. The displacements u of other nodes of the cross-section are dependent of u_A and u_B. Eq. (20) shows that displacement v is systematically equal to zero, so this equation is applied at all the nodes of the model. Concerning the displacements w, Eq. (21) is applied at all nodes of the cross-sections, except point A. The displacement component w of other nodes is in the same way dependent of w_A. This description shows that the methodology relies on slave and master degrees of freedom. For the sake of simplicity, one distinguishes between master and slave nodes. A given node is considered as a master node if it contains at least one master degree of freedom. This model contains three master degrees of freedom per cross-section. It can be observed that Eq. (21) defines linear relations between the slave and the master degrees of freedom. One complementary remark is that if two master nodes are needed, it is natural to select points A and B. But two other nodes could be selected as well, which leads to equivalent results.

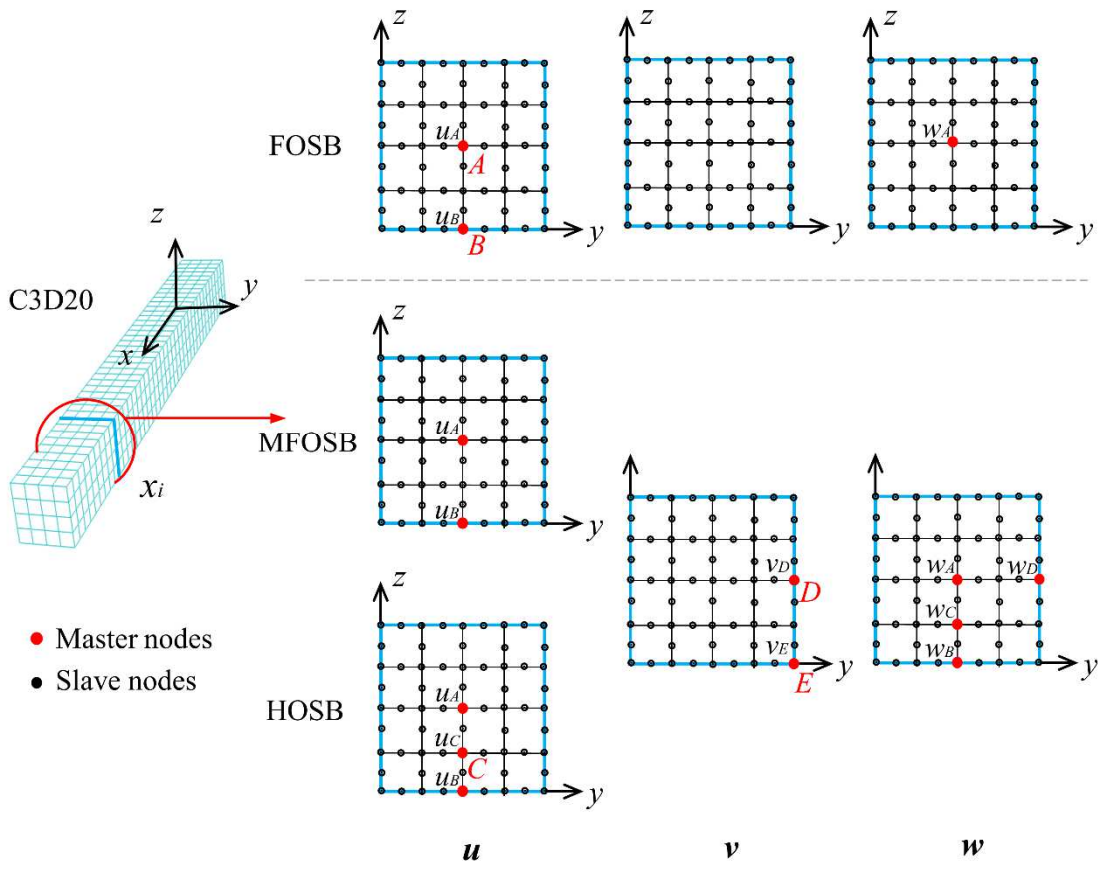

Fig. 3. Master nodes and slave nodes on a cross-section of a solid-beam model.

3.2 MFOSB model

The methodology described in Section 3.1 is now applied to build the MFOSB model. This model exploits five master nodes A, B, C, D and E, as shown in Fig. 3. Eq. (14) contains two coefficients (a_1 and a_2) to be determined for displacement u, two coefficients (b_1 and b_2) for displacement v and three coefficients (c_1 , c_2 , c_3 and c_4) for displacement w. The coefficients

a_1 and a_2 are the same as the FOSB model. To identify other coefficients, the following equations are used:

$$\begin{cases} v(y_D, z_D) = v_D = y_D z_D b_1 + y_D b_2 \\ v(y_E, z_E) = v_E = y_E z_E b_1 + y_E b_2 \\ w(y_A, z_A) = w_A = z_A^2 c_1 + y_A^2 c_4 + z_A c_2 + c_3 \\ w(y_B, z_B) = w_B = z_B^2 c_1 + y_B^2 c_4 + z_B c_2 + c_3 \\ w(y_C, z_C) = w_C = z_C^2 c_1 + y_C^2 c_4 + z_C c_2 + c_3 \\ w(y_D, z_D) = w_D = z_D^2 c_1 + y_D^2 c_4 + z_D c_2 + c_3 \end{cases} \quad (22)$$

where $v_D,\ v_E,\ w_A,\ w_B,\ w_C$ and w_D are displacements at master nodes; $y_A,\ y_B,\ y_C,\ y_D,\ y_E,$ $z_A,\ z_B,\ z_C,\ z_D$ and z_E are the coordinates of master nodes in the *y* or *z* direction.

The expressions of coefficients identified for each cross-section are shown in Appendix A.

Considering the equation in Appendix A and replacing *y* and *z* by y_i and z_i in Eq. (14), one obtains linear equations to be applied at slave node *i*:

$$\begin{cases} u(y_i, z_i) = u_i^S = z_i a_1 + a_2 \\ v(y_i, z_i) = v_i^S = y_i z_i b_1 + y_i b_2 \\ w(y_i, z_i) = w_i^S = z_i^2 c_1 + y_i^2 c_4 + z_i c_2 + c_3 \end{cases} \quad (23)$$

The MFOSB model contains eight master degrees of freedom per cross-section. Eq. (23) describes linear relations between slave and master degrees of freedom.

3.3 HOSB model

The methodology is now applied to build the HOSB model. This model exploits five master nodes *A*, *B*, *C*, *D* and *E*, as shown in Fig. 3. Eq. (17) contains three coefficients (a_1, a_2 and a_3) to be determined for displacement *u*, two coefficients (b_1 and b_2) for displacement *v* and four coefficients (c_1, c_2, c_3 and c_4) for displacement *w*. To identify the nine coefficients, the following equations are used:

$$\begin{cases} u(y_A, z_A) = u_A = a_1 z_A^3 + a_2 z_A + a_3 \\ u(y_B, z_B) = u_B = a_1 z_B^3 + a_2 z_B + a_3 \\ u(y_C, z_C) = u_C = a_1 z_C^3 + a_2 z_C + a_3 \\ v(y_D, z_D) = v_D = y_D z_D b_1 + y_D b_2 \\ v(y_E, z_E) = v_E = y_E z_E b_1 + y_E b_2 \\ w(y_A, z_A) = w_A = z_A^2 c_1 + y_A^2 c_4 + z_A c_2 + c_3 \\ w(y_B, z_B) = w_B = z_B^2 c_1 + y_B^2 c_4 + z_B c_2 + c_3 \\ w(y_C, z_C) = w_C = z_C^2 c_1 + y_C^2 c_4 + z_C c_2 + c_3 \\ w(y_D, z_D) = w_D = z_D^2 c_1 + y_D^2 c_4 + z_D c_2 + c_3 \end{cases} \quad (24)$$

where $u_A,\ u_B,\ u_C, v_D,\ v_E,\ w_A,\ w_B,\ w_C$ and w_D are the displacements at master nodes; $y_A,$

y_B, y_C, y_D, y_E, z_A, z_B, z_C, z_D and z_E are the coordinates of master nodes.

The expressions of coefficients b_1, b_2, c_1, c_2, c_3 and c_4 are the same as expressed in Appendix A, coefficients a_1, a_2 and a_3 identified for each cross-section are:

$$\begin{cases} a_1 = \dfrac{u_A z_B - u_B z_A - u_A z_C + u_C z_A + u_B z_C - u_C z_B}{(z_A - z_B)(z_A^2 z_B - z_A^2 z_C + z_A z_B^2 - z_A z_B z_C - z_B^2 z_C + z_C^3)} \\ a_2 = -\dfrac{u_A z_B^3 - u_B z_A^3 - u_A z_C^3 + u_C z_A^3 + u_B z_C^3 - u_C z_B^3}{(z_A - z_B)(z_A^2 z_B - z_A^2 z_C + z_A z_B^2 - z_A z_B z_C - z_B^2 z_C + z_C^3)} \\ a_3 = -\dfrac{-u_C z_A^3 z_B + u_B z_A^3 z_C + u_C z_B^3 z_A - u_B z_C^3 z_A + u_A z_B^3 z_C - u_A z_C^3 z_B}{(z_A - z_B)(z_A^2 z_B - z_A^2 z_C + z_A z_B^2 - z_A z_B z_C - z_B^2 z_C + z_C^3)} \end{cases} \quad (25)$$

After considering the equation in the Appendix A and Eq. (25) and replacing *y* and *z* by y_i and z_i in Eq. (17), one obtains linear equations to be applied at slave node *i*:

$$\begin{cases} u(y_i, z_i) = u_i^S = z_i^3 a_1 + z_i a_2 + a_3 \\ v(y_i, z_i) = v_i^S = y_i z_i b_1 + y_i b_2 \\ w(y_i, z_i) = w_i^S = z_i^2 c_1 + y_i^2 c_4 + z_i c_2 + c_3 \end{cases} \quad (26)$$

The HOSB model contains nine master degrees of freedom per cross-section. Eq. (26) describes linear relations between slave and master degrees of freedom.

3.4 Synthesis

The method is the same for the three beam theories considered in Sections 3.1 to 3.3. The only difference is the number of master degrees of freedom per cross-section, namely three, eight and nine for the FOSB, MFOSB and HOSB models respectively as shown in Table 1. The number of equations applied is equal to the number of slave degrees of freedom which are eliminated. Consequently, the model size does not depend on the number of nodes in each cross-section but is given by the number of master degrees of freedom.

Table 1. For each cross-section, number of master nodes and master degrees of freedom for the three solid-beam models and a 2D beam model.

	FOSB	MFOSB	HOSB	2D Beam element
Number of master degrees of freedom	*u*: 2 *v*: 0 *w*: 1 total: **3**	*u*: 2 *v*: 2 *w*: 4 total: **8**	*u*: 3 *v*: 2 *w*: 4 total: **9**	*u*, *w*, θ_y total: **3**
Number of corresponding master nodes	2	4	5	1

This new solid-beam approach uses displacements exclusively, without rotations or other types of degrees of freedom. It is an interesting characteristic of our methodology, particularly for higher-order theories that initially use not only displacements and rotations but also other types

of degrees of freedom. Moreover, other displacement fields can also be applied in our approach, for instance, an even higher-order beam theory can be considered if necessary.

4 Examples

4.1 Straight beam with square cross-section under distributed loading

4.1.1 Presentation of the example

The straight beam with square cross-section is presented in Fig. 4. The structure is clamped at its two ends and submitted to a distributed loading applied on the upper surface. A relatively thin beam case (l/h=20) as well as a thick beam one (l/h=5), are considered.

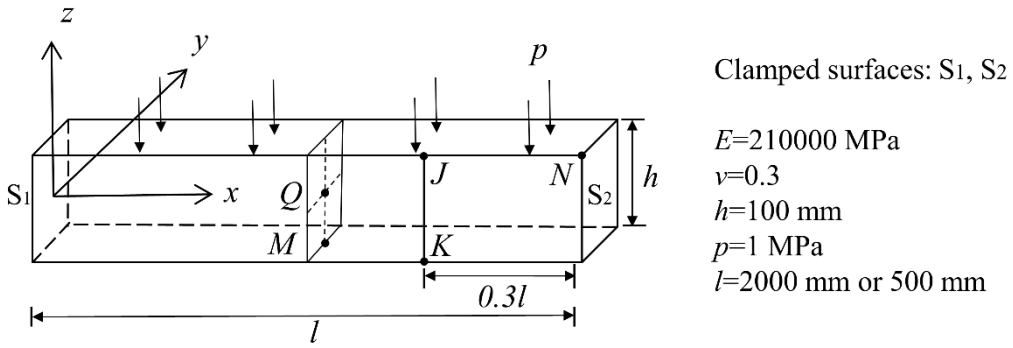

Fig. 4. Straight beam with square cross-section under distributed loading − Presentation of the example.

4.1.2 Convergence study

A convergence study with different l/h ratios is presented, to ensure that solid-beam approach meets the convergence conditions and to compare its performances with those of the solid approach. In this example, the twenty-node hexahedral finite element C3D20 of Abaqus [39] is used. The displacement for several mesh refinement levels is observed at the center (point M in Fig. 4) of the bottom surface. The solid models with very fine 8×8×100 and 8×8×60 meshes are respectively chosen as the reference for thin and thick cases. Convergence is considered to be achieved if the error is less than 0.5% compared with these reference models. The results of thin and thick cases are reported in Fig. 5. The solid model and the HOSB model give very close results and convergence is obtained with a 4×4×40 mesh in the thin case and a 4×4×20 mesh in the thick one. The MFOSB model is satisfactory in the thin case but leads to a small error in the thick one, even for a refined mesh. The FOSB model converges to completely wrong values compared with the reference solid model. Consequently, this model is unacceptable.

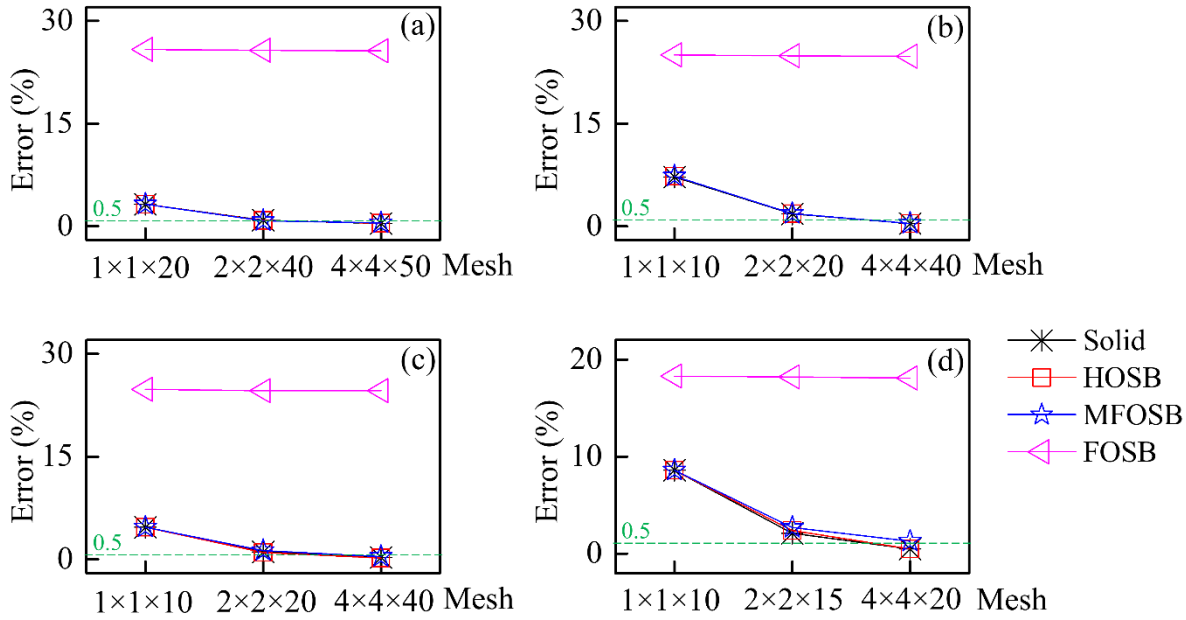

Fig. 5. Straight beam with square cross-section under distributed loading – Convergence study of displacement w at point M for different l/h ratios. (a) l/h =1000 (b) l/h =100 (c) l/h =20 (d) l/h =5.

4.1.3 Displacements and stresses in the thin case

Even if slave nodes have been eliminated from the system of equations to be solved, displacements are available at all nodes. Then the stresses can be calculated in all the elements. The average value at nodes is retained to evaluate the stresses. First displacements as well as von Mises stresses are observed over the whole structure. Results from a solid model are always chosen as the reference to evaluate our solid-beam models in this paper. The comparison of the results between solid, HOSB and MFOSB models are presented in Fig. 6. The FOSB model is not considered because its convergence performance is not satisfactory. These results are obtained with the 4×4×40 mesh, which meets the convergence criterion as highlighted in Section 4.1.2. The vertical displacements and von Mises stresses obtained with the three models are very similar to each other.

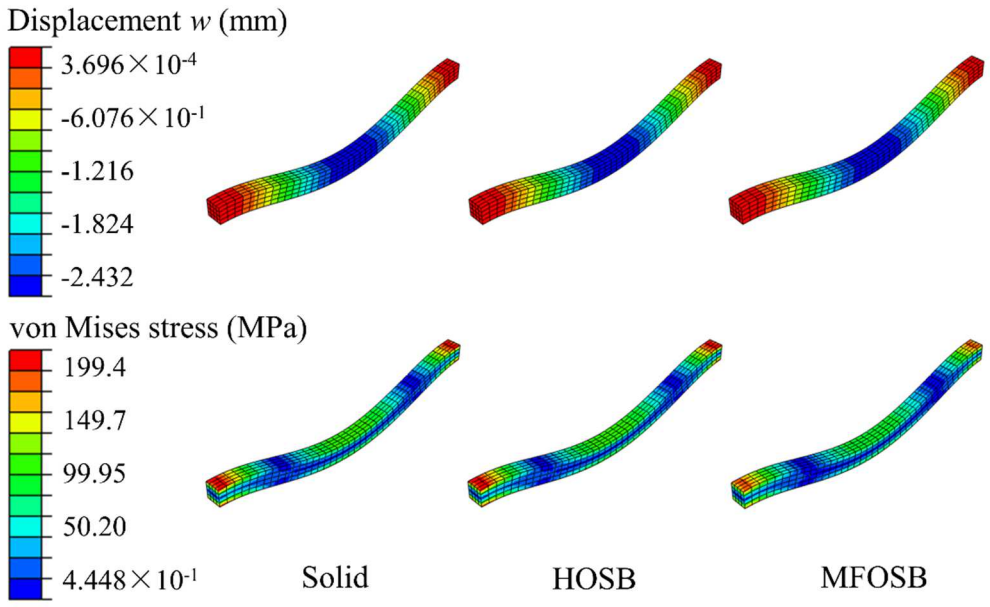

Fig. 6. Straight beam with square cross-section under distributed loading – Displacement *w* and von Mises stress distribution in the thin case.

The distribution of vertical displacement along the mid-axis and von Mises stress along a line on the lower surface is shown in Fig. 7. The solid-beam models are compared with the solid model and two classical beam models. The elements B21 and B23 in Abaqus are used for representing the thick beam and thin beam models respectively. A mesh containing forty B21 or B23 finite elements, which meets the convergence criterion, is considered for the thin beam and thick beam models. All the models have similar results for displacements and stresses except the FOSB model which shows significant errors. These errors are essentially due to a spurious σ_{zz} stress state being discussed below.

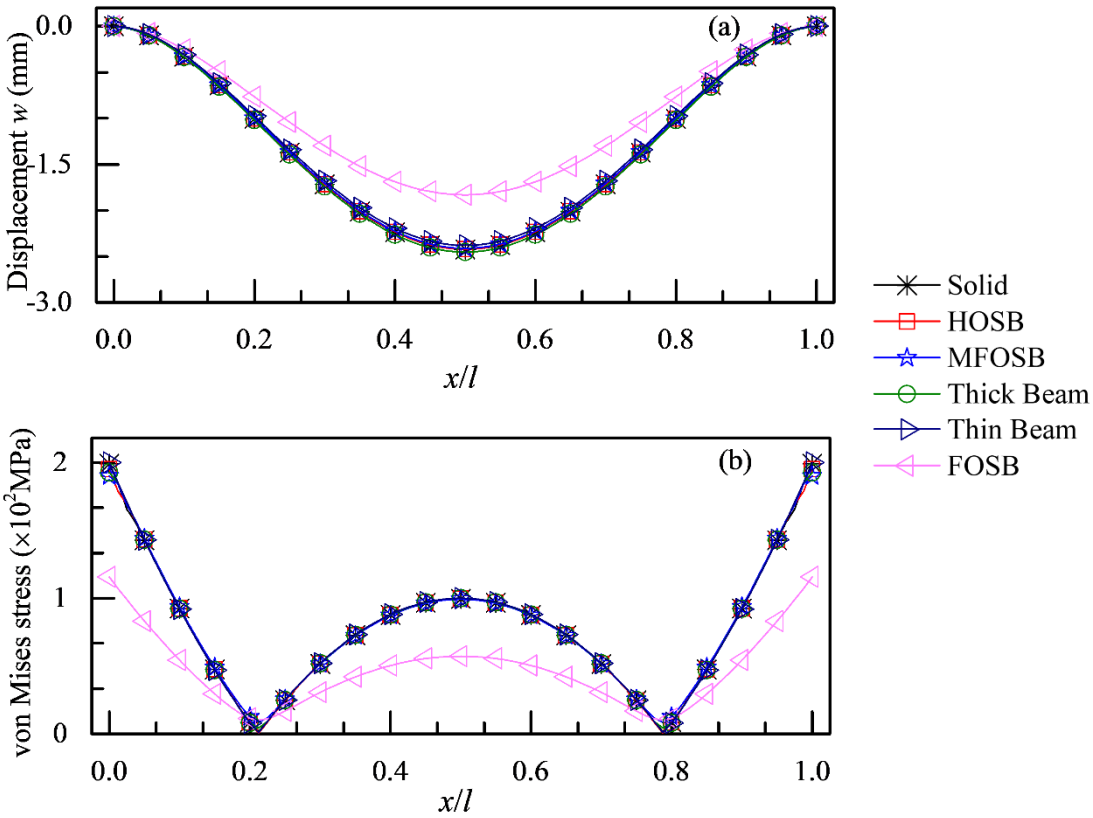

Fig. 7. Straight beam with square cross-section under distributed loading – Distribution of vertical displacement along the mid-axis (a) and von Mises stress along a line on the lower surface (b), in the thin case.

Fig. 8 presents the through-the-thickness distribution of displacements and stresses along a line *JK* (see Fig. 4). The solid model is considered as the reference. Firstly, the FOSB model shows unsatisfactory results, especially for displacement *w* (Fig. 8b) and σ_{zz} stress (Fig. 8e). Because *w* is considered as constant through the thickness, the ε_{zz} strain is equal to zero, which is not correct due to the Poisson effect. In the same way, *v* is equal to zero in the FOSB model and this is also in contradiction with the Poisson effects. These nonphysical assumptions greatly disturb the state of stress in the 3D elasticity situation. Particularly, it implies large σ_{zz} stress, which should remain very small in this thin beam case. Therefore, the von Mises stress depending on the different stress components is affected and this explains the bad results reported in Fig.7. These poor results confirm that this kinematic assumption is not compatible with 3D theory of elasticity, although consistent and valid in the context of the classical beam theory. Furthermore, the FOSB model also gives a constant σ_{xz} stress distribution (Fig. 8d), which is a well-known limitation of the Timoshenko beam theory. Usually, the integration of equilibrium equations is used to obtain a quadratic and correct distribution of transverse shear stresses.

The reference displacement *u* (Fig. 8a) is linear and both the MOFSB and HOSB models perfect fit this distribution. The displacement *w* is also well predicted by these two solid-beam models. This component seems to be constant but actually has a slight quadratic tendency. One can observe linear distribution of σ_{xx} stress (Fig. 8c) and again the MOFSB and HOSB models

provide good results. The HOSB model accurately reproduces the classical quadratic distribution of σ_{xz} stress. Namely, the free-face condition $\sigma_{xz} = 0$ is almost met at top and bottom surfaces. Thanks to the quadratic distribution of displacement *w*, the MFOSB model also exhibits a quadratic trend, but a significant discrepancy with the reference result is observed. Namely the free-face condition mentioned above is not met. However, it is not important for this thin case since transverse shear stresses are usually neglected in thin structures and the influence of transverse shear effects on displacements is small. In summary the HOSB model gives outstanding results for the thin case, while the MOFSB model is also satisfactory but cannot perfectly reproduce the transverse shear effects. Anyway, one can neglect these effects for a thin structure. Finally, the FOSB model is not able to provide good results, and thus is not considered for the rest of the study.

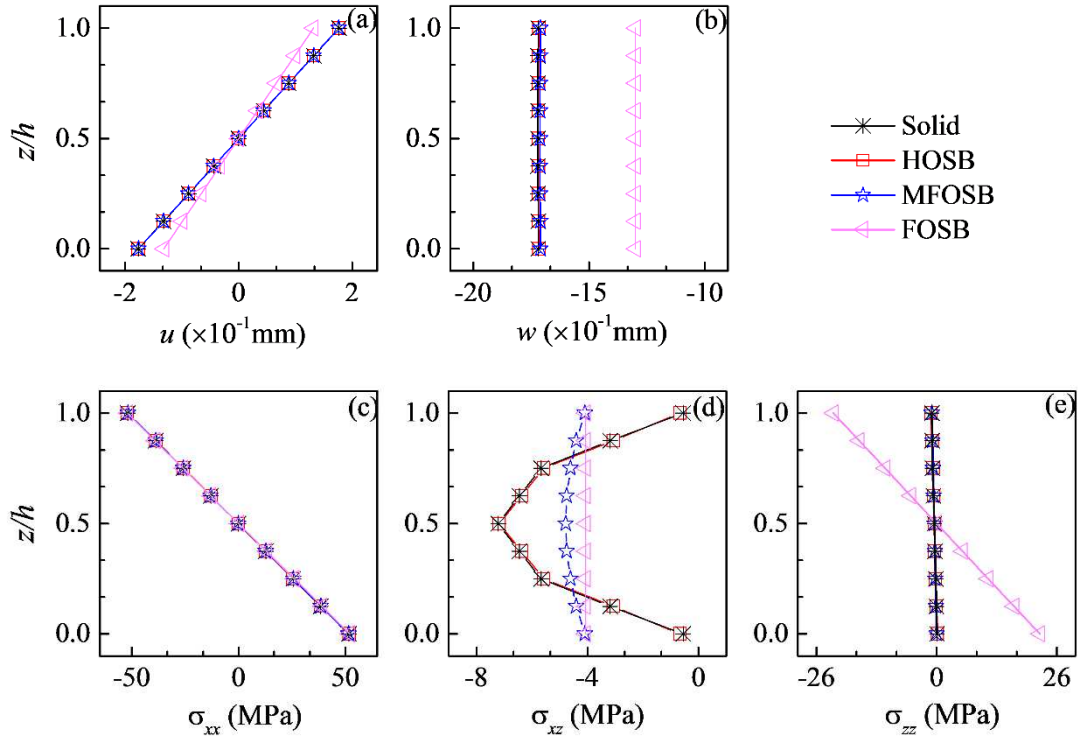

Fig. 8. Straight beam with square cross-section under distributed loading – Through-the-thickness displacement and stresses along a line *JK*, in the thin case.

4.1.4 Displacements and stresses in the thick case

As for the thin case, first of all, displacements and von Mises stresses are observed over the whole structure. The comparison of results obtained with the solid, MOFSB and HOSB models are shown in Fig. 9. The 4×4×20 mesh, which meets the convergence criterion as highlighted in Section 4.1.2, is used. The solid model and the HOSB model perform similar results in this global observation. For the MOFSB model, some little difference appears on displacement and von Mises stress in this thick beam case.

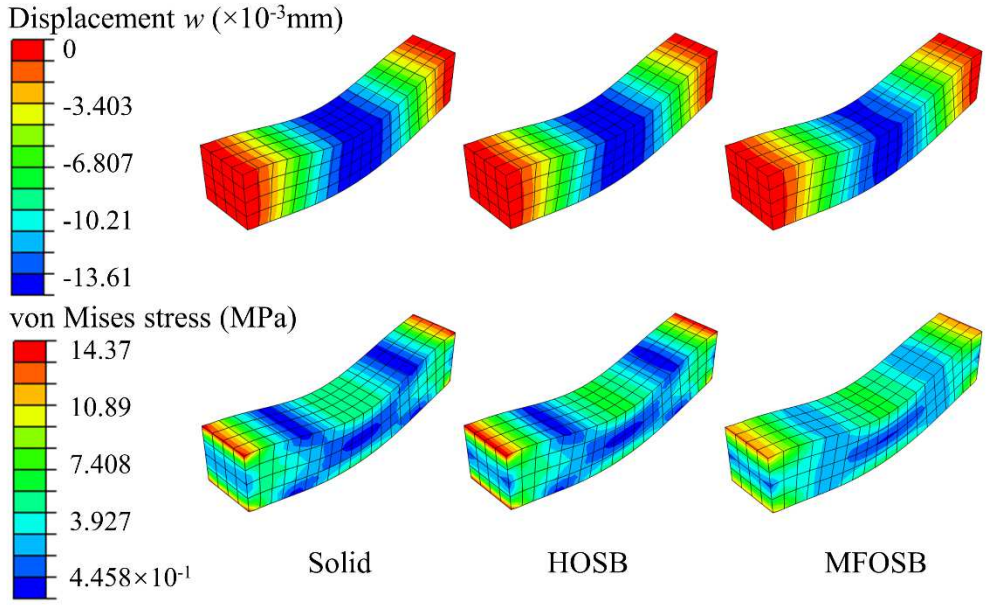

Fig. 9. Straight beam with square cross-section under distributed loading – Displacement w and von Mises stress distribution in the thick case.

Fig. 10 presents the distribution of vertical displacement along the mid-axis and von Mises stress along a line on the lower surface. The solid model and solid-beam models use the 4×4×20 mesh, while the beam models use a mesh with twenty elements, which both satisfy the convergence criterion. For displacement, the HOSB model fits very well with the solid one. Significant error is obtained with the thin beam model which neglects transverse shear effects. Relatively small errors appear with the thick beam model and the MFOSB model. For von Mises stress, again the HOSB model has a perfect fit with the reference, while the beam models lead to small errors in the boundary conditions area. The discrepancy shown with the MFOSB model is due to a rough calculation of transverse stresses which play a significant role in thick structures. Therefore, the HOSB model is confirmed to properly predict the mechanical behavior of a thick beam which is submitted to significant transverse shear effects.

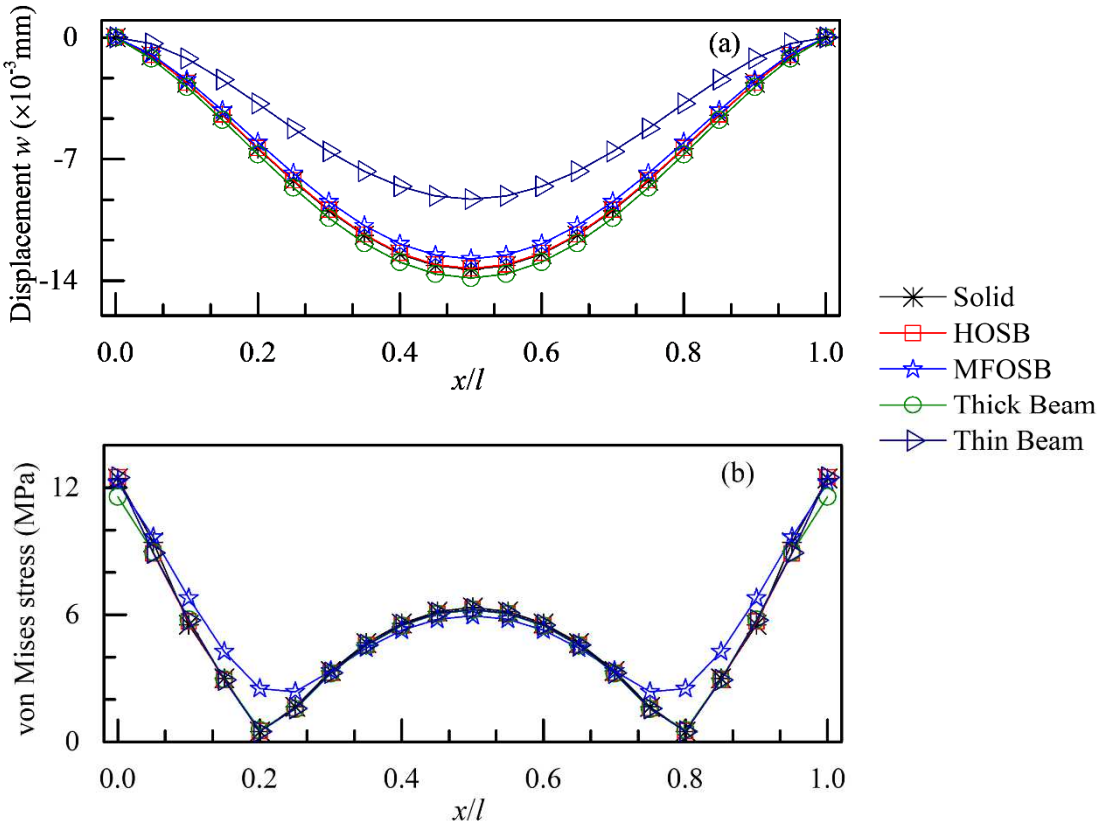

Fig. 10. Straight beam with square cross-section under distributed loading – Distribution of vertical displacement along the mid-axis (a) and von Mises stress along a line on the lower surface (b), in the thick case.

Fig. 11 shows the distribution of displacements and stresses along a line *JK* (see Fig. 4), again the solid model being the reference. Several limitations are shown with the MFOSB model. The quadratic tendency of displacement *w* (Fig. 11b) is reproduced but the values are incorrect, which means the stiffness is not well estimated. This is due to the fact that transverse shear stiffness is not precisely calculated. Namely, this model fails in reproducing the quadratic distribution of the reference stress σ_{xz} (Fig. 11d). Moreover, the free-face condition $\sigma_{xz} = 0$ is not met at top and bottom surfaces. And obviously, the transverse shear effects play an important role in the thick case. The classical Timoshenko beam theory is associated with shear correction factors to avoid the limitation caused by kinematic assumptions. But in our solid-beam approach, no correction factor is introduced. Of course, this wrong σ_{xz} distribution consequently leads to errors on the von Mises stress, as highlighted in Fig. 10. Besides, this MFOSB model cannot replicate the slight nonlinear distribution of displacement *u* (Fig. 11a) and stress σ_{xx} (Fig. 11c). On the contrary, the HOSB model shows an excellent fit with the solid model. It correctly predicts the quadratic distribution of displacement *w*, the nonlinear distribution of stress σ_{xx} and the quadratic distribution of stress σ_{xz}. In particular, the free-face condition $\sigma_{xz} = 0$ is almost met at top and bottom surfaces. Moreover the distribution of stress σ_{zz} (Fig. 11e) is also correctly predicted.

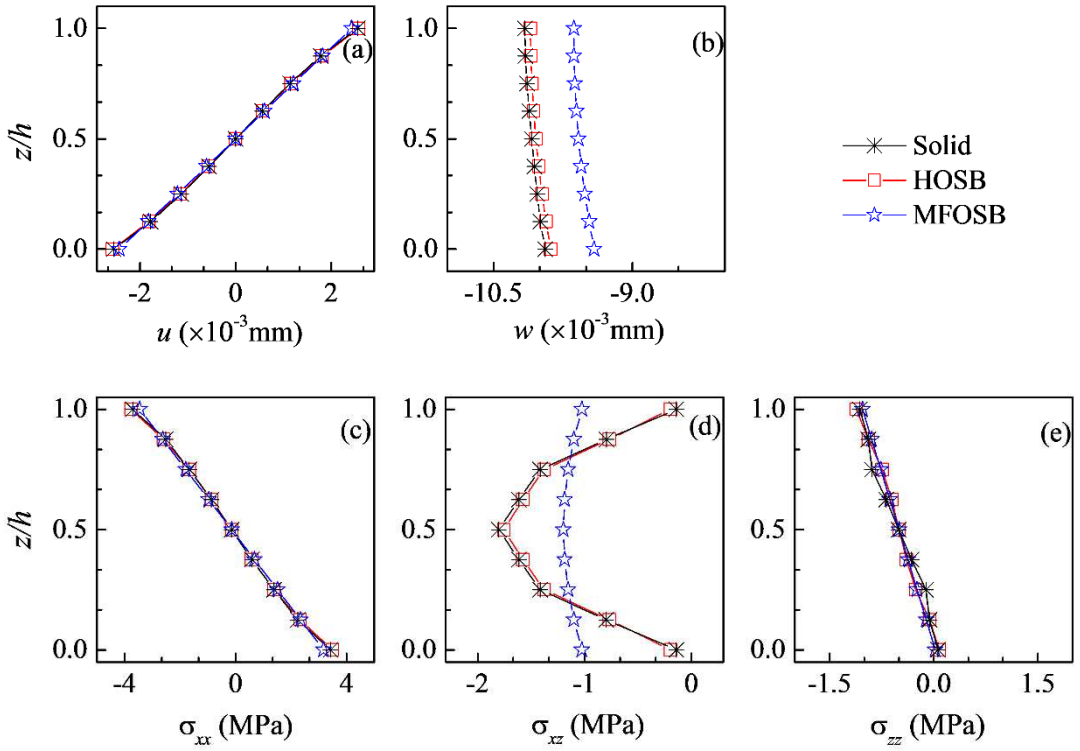

Fig. 11. Straight beam with square cross-section under distributed loading – Through-the-thickness displacement and stresses along a line *JK*, in the thick case.

4.1.5 Accuracy synthesis of solid-beam models

Table 2 summarizes the errors obtained with the solid-beam models in the thin and thick cases. These errors are calculated at center (point *Q* in Fig. 4) and corner (point *N* in Fig. 4) corresponding to the maximal displacement and von Mises stress respectively. The MFOSB model shows good performance in the thin case, the maximal error being limited to about 1% for the displacement and von Mises stress. The HOSB model even works better because transverse shear effects are not completely negligible in this thin case. Actually, the *l*/*h* ratio equaling to 20 is not characteristic of a very thin beam. For the thick case, the HOSB model remains satisfactory with errors not exceeding 1.5%. The MFOSB model is less efficient, errors are close to 5% for the displacement and 9% for the von Mises stress. Summarily, the MFOSB model is convenient for the thin case only, while the HOSB model gives excellent results in both the thin and thick cases. Additionally, the same study has been performed with the eight-node hexahedral element C3D8I of Abaqus. Similar results have been obtained showing that the solid-beam methodology can be used with any efficient solid element.

Table 2. Straight beam with square cross-section under distributed loading – Errors on maximal displacement and maximal von Mises stress.

Examples	Models	Displacement w		von Mises stress	
		Maximum ($\times 10^{-2}$mm)	Error (%)	Maximum (MPa)	Error (%)
Thin case	Solid	-243.2	–	184.5	–
	HOSB	-242.9	0.1	183.6	0.5
	MFOSB	-242.0	0.5	182.4	1.1
Thick case	Solid	-1.361	–	11.76	–
	HOSB	-1.355	0.4	11.59	1.4
	MFOSB	-1.299	4.6	10.76	8.5

4.2 Curved beam with square cross-section under distributed loading

4.2.1 Presentation of the example

The second example is a curved beam with a square cross-section. The structure is clamped at its two ends and submitted to a distributed vertical loading applied on the top surface, as shown in Fig. 12a. A relatively thin beam case (r/h=10) as well as a thick beam one (r/h=10/3), are considered. This structure is curved, which leads to the coupling of bending and membrane effects, compared with the first example for which the structure is submitted to pure bending effects only. Furthermore, local coordinate systems (see in Fig. 12b) are created for each cross-section to apply kinematic relations.

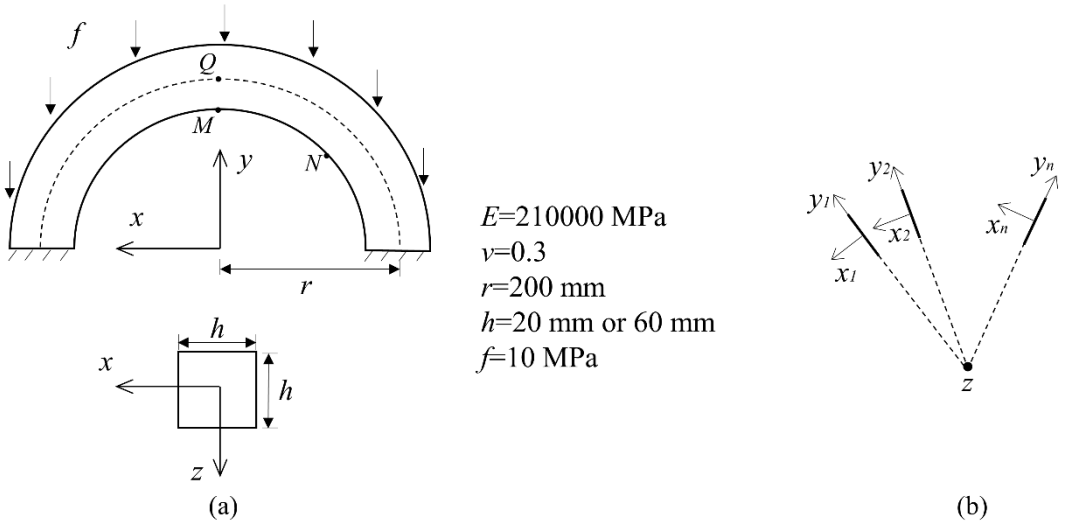

Fig. 12. Curved beam with square cross-section under distributed loading – Presentation of the example.

4.2.2 Convergence study

The same type of convergence study detailed in Section 4.1.2 is presented here. Again, the element C3D20 is used. The evolution of displacement for different mesh refinement levels at point M (see Fig. 12a) is observed. A solid model with a very fine 8×8×100 mesh is chosen to

be a reference. The convergence is considered to be achieved if the error is less than 0.5% compared with the reference. The results of thin and thick cases are reported in Fig 13. The observations are similar, compared to the first example. The solid model and the HOSB model give very close results and convergence is obtained with a 4×4×50 mesh in the thin and thick cases. The MFOSB model is satisfactory in the thin case but leads to a small error in the thick one, even for a refined mesh.

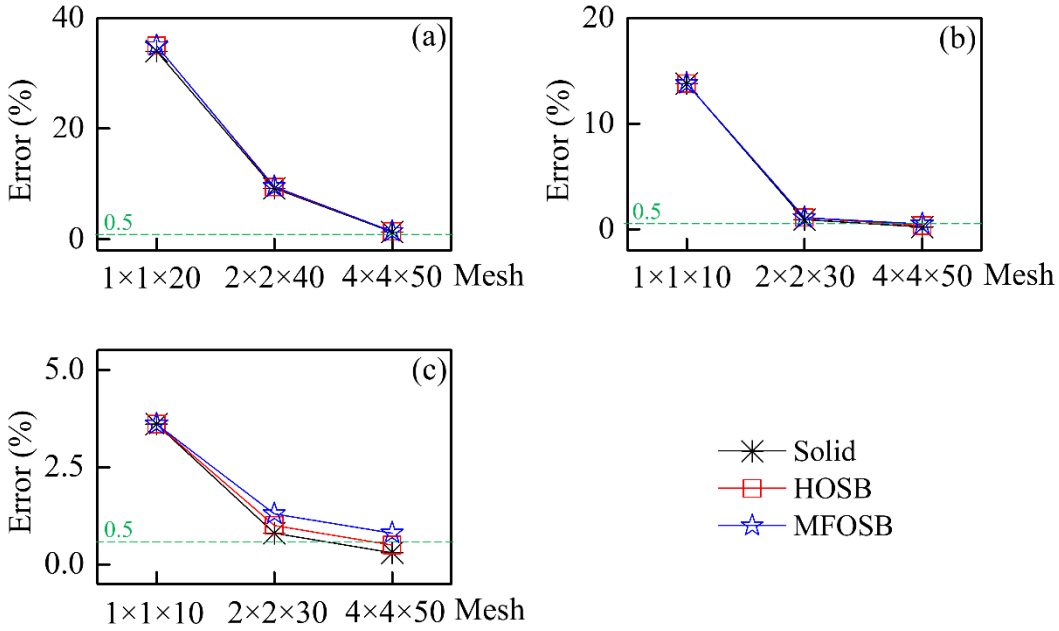

Fig. 13. Curved beam with square cross-section under distributed loading – Convergence study of displacement w at point M for different r/h ratios. (a) r/h =100 (b) l/h =10 (c) l/h =10/3.

4.2.3 Displacements and stresses in the thin case

Displacement w and von Mises stress are observed over the whole structure. Fig. 14 shows a comparison of results between the solid, MFOSB and HOSB models. The results are obtained with the 4×4×50 mesh, which meets the convergence criterion. Similar displacements and von Mises stress results are obtained with the three models.

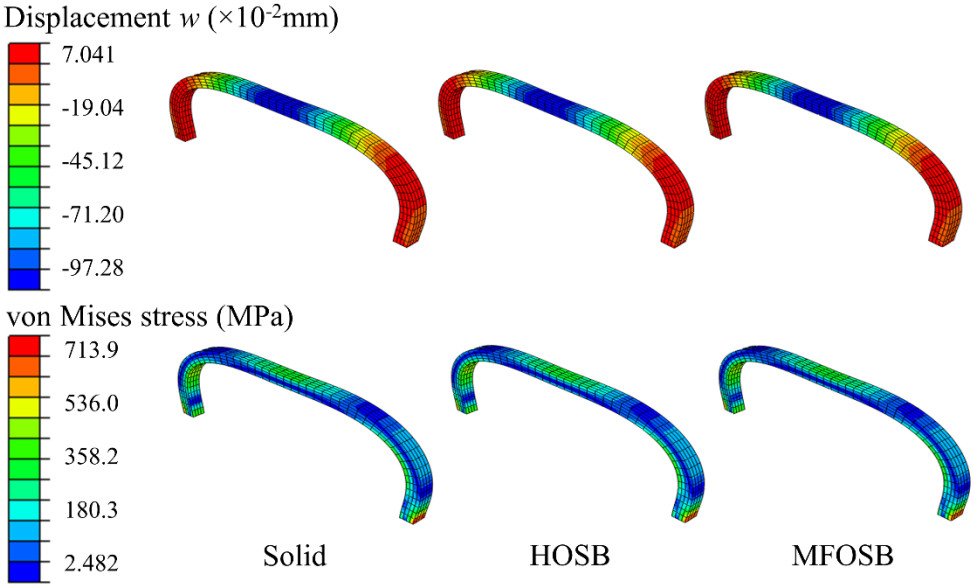

Fig. 14. Curved beam with square cross-section under distributed loading – Displacement and von Mises stress distributions in the thin case.

Fig. 15 presents the distribution of vertical displacement in the global coordinate system along the mid-axis and von Mises stress along a line on the lower surface. Again the 4×4×50 mesh is chosen for the solid and solid-beam models. For the thin beam and thick beam models, a mesh containing fifty elements is considered. Almost all the models give similar results of displacements and von Mises stress. The thin beam model leads to some minor difference compared with the reference. Indeed, the structure is not very thin and consequently, transverse shear effects, which are not taken into account by in the thin beam theory, are not completely negligible.

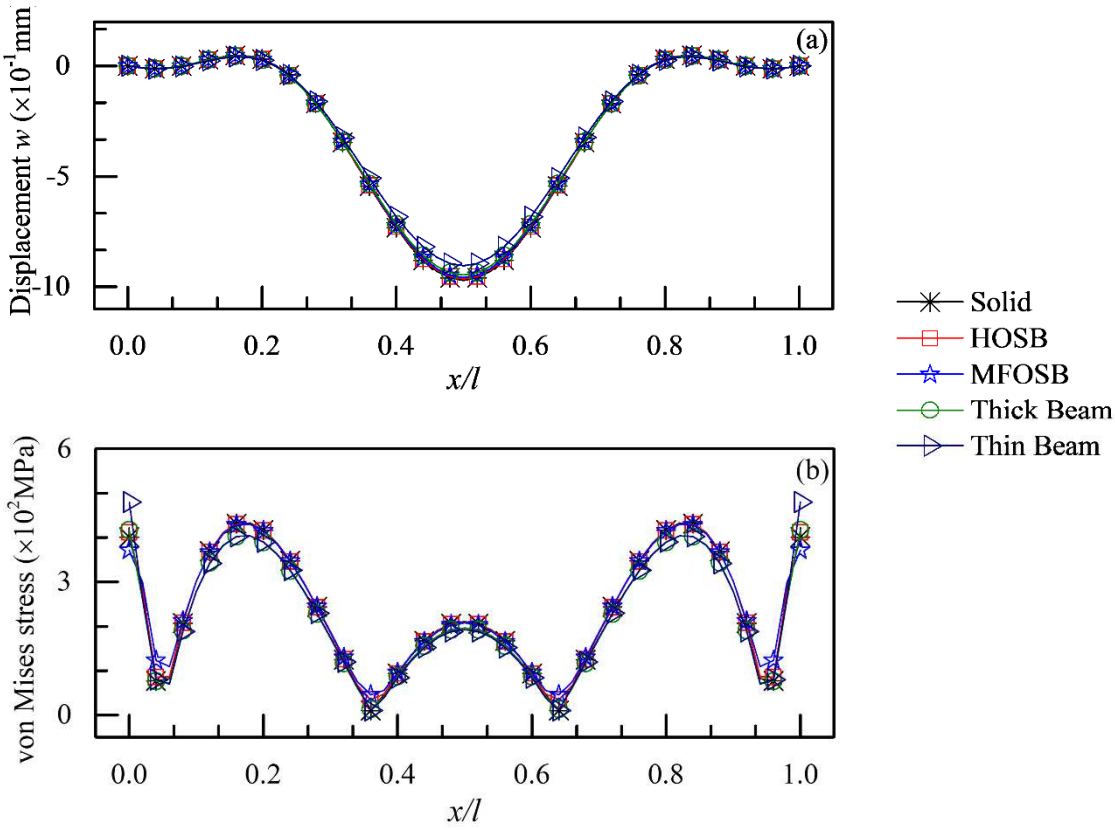

Fig. 15. Curved beam with square cross-section under distributed loading – Distribution of vertical displacement along the mid-axis (a) and von Mises stress along a line on the lower surface (b), in the thin case.

4.2.4 Displacements and stresses in the thick case

As for the thin case displacements and von Mises stresses are observed over the whole structure. Fig. 16 shows a comparison of results obtained with solid, MFOSB and HOSB models. The 4×4×50 mesh, which meets the convergence criterion, is used. The three models show close results, some minor differences on displacements and von Mises stresses can be observed.

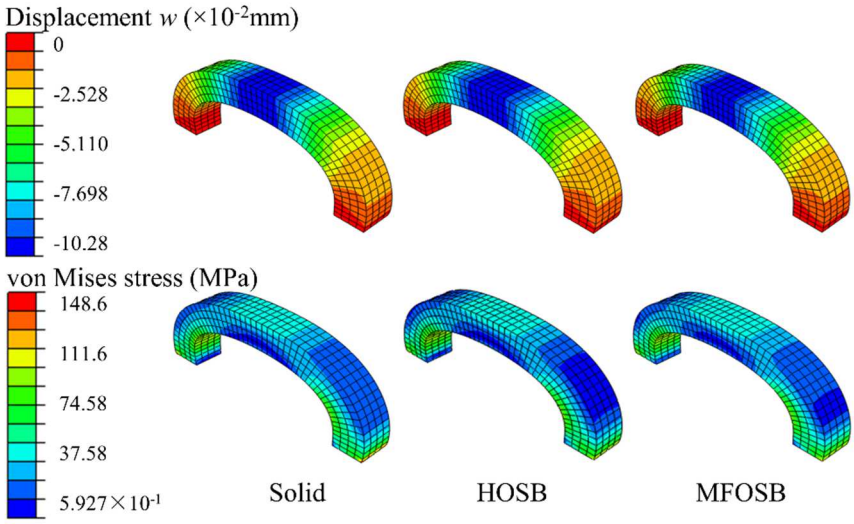

Fig. 16. Curved beam with square cross-section under distributed loading – Displacement and von Mises stress distributions in the thick case.

Fig. 17 gives the distribution of vertical displacement in the global coordinate system along the mid-axis and von Mises stress along a line on the lower surface. The solid model is considered as a reference. Again the 4×4×50 mesh is used for the solid and solid-beam models. For the beam models, a mesh containing fifty elements is used. The HOSB model fits well with the solid one for displacement, while some minor error is found with the MFOSB model. The HOSB model gives excellent result for von Mises stress, but the MFOSB model leads to some errors. These results confirm that the HOSB model is necessary to better reproduce the transverse shear effects which are significant in the thick beam case. It is worth mentioning that in this thick curved beam case, the thin beam model gives bad displacement and von Mises stress results. Moreover, even the thick beam model appears unsatisfactory for calculating von Mises stress. In Fig. 12a, one can see that the distributed loading is applied on the upper face of the structure. This is correctly taken into account with a solid or solid-beam model, but in the beam models, loading is applied on the mid-axis, except if specific techniques are used. For a curved and thick structure, the length of the mid-axis is significantly different from the length of the line on the upper face, leading to a loading error. It is a limitation of the beam approach and so the solid-beam approach is preferable from this point of view.

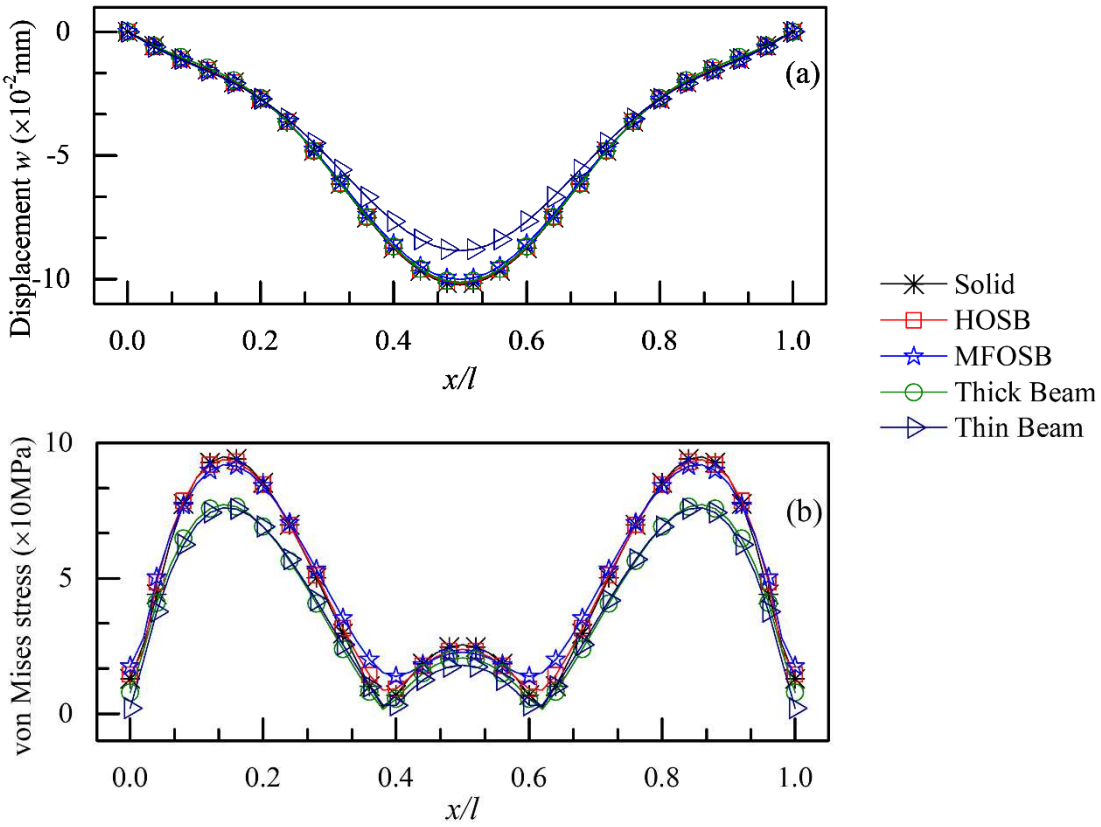

Fig. 17. Curved beam with square cross-section under distributed loading – Distribution of vertical displacement along the mid-axis (a) and von Mises stress along a line on the lower surface (b), in the thick case.

4.2.5 Accuracy synthesis of solid-beam models

Table 3 summarizes the errors obtained with the solid-beam models, in the thin and thick curved beam cases. These errors are calculated at center (point *Q* in Fig. 12a) and point *N* (in Fig.12a) for displacement and von Mises stress, corresponding to the maximal displacement and von Mises stress respectively. The MFOSB model gives good results in the thin case, with errors around 1% for the displacement and von Mises stress. Similar to the first example, the HOSB model performs better. In the thick case, the HOSB model remains satisfactory with the errors limited to about 1%. The MFOSB model leads to some discrepancy, but the errors: about 2% for displacement and 3% for von Mises stress, remain limited. In summary, the HOSB model gives excellent results in both the thin and thick cases, while the MFOSB model is convenient for thin structures only. Again, similar results have been obtained by element C3D8I, which confirms that the methodology can be exploited with any efficient solid finite element.

Table 3. Curved beam with square cross-section under distributed loading – Errors on maximal displacement and maximal von Mises stress.

Examples	Models	Displacement w		von Mises stress	
		Maximum ($\times 10^{-2}$mm)	Error (%)	Maximum (MPa)	Error (%)
Thin curved beam	Solid	-97.28	–	432.6	–
	HOSB	-96.75	0.5	430.6	0.5
	MFOSB	-96.03	1.2	429.7	0.7
Thick curved beam	Solid	-10.34	–	94.92	–
	HOSB	-10.28	0.6	93.86	1.1
	MFOSB	-10.11	2.2	91.95	3.2

4.3 Model size

Fig. 18 compares the number of degrees of freedom between the solid model, and our solid-beam models. The results are obtained for the thin straight beam example, but other examples share the same trends. The size reduction is due to equations which lead to an elimination of slave degrees of freedom. It is an expected and hopeful characteristic of the solid-beam approach that the reduction of the number of degrees of freedom increases with the number of elements. For fine meshes, the gain is significant with solid-beam models compared with reference solid models. As highlighted in Section 4.1.2 dealing with the convergence study, for the solid model as well as solid-beam models, the 4×4×40 mesh is necessary to obtain sufficiently precise results in terms of displacements and stresses. Of course, the gain of the MFOSB model is slightly larger compared with the HOSB model due to a smaller number of master nodes.

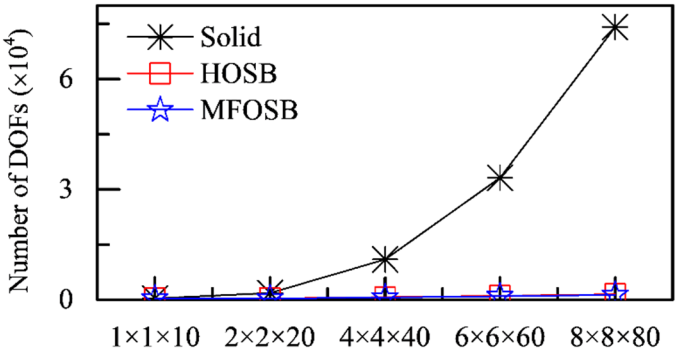

Fig. 18. Influence of the meshing refinement level on the number of degrees of freedom between solid, HOSB and MFOSB models.

It's interesting to compare the MFOSB and HOSB models with classical beam elements in terms of computational cost. Fig. 19 presents the comparison of the number of degrees of freedom for the curved beam example. For the solid-beam models, the results are reported with a 4×4×50 mesh which meets the convergence condition. The beam model with the same refinement level along the length of the structure is also considered, to compare the solid-beam

approaches and the beam one. Results confirm that the beam or solid-beam approach gives a significant gain compared with the solid approach. In terms of model size and consequently of computational time, the solid-beam models are comparable with the beam models. It can also be observed that the HOSB model requires only a little more degrees of freedom than the MFOSB model.

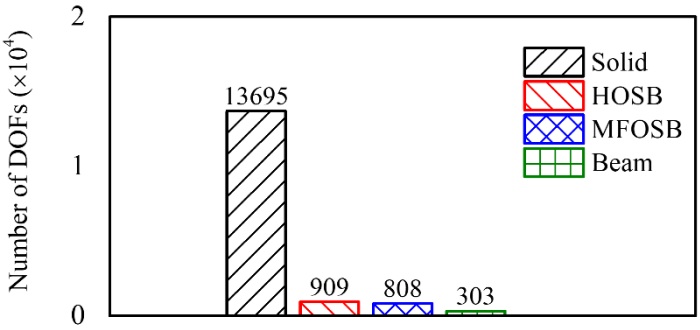

Fig. 19. Comparison of the number of degrees of freedom between solid, HOSB, MFOSB and beam models.

5 Conclusion

A new solid-beam approach dedicated to thin to thick beam structures under bending and membrane effects has been presented. Beam displacement fields are directly applied on a solid finite element model which contains several elements through the thickness and the width of the cross-section. Three theories based on kinematic assumptions are considered. The classical first-order Timoshenko theory, a modified first-order beam theory and a higher-order beam theory lead to the FOSB, the MFOSB and the HOSB models respectively. The methodology relies on the slave and master nodes technique. Kinematic relations are imposed at slave nodes throughout the cross-sections to meet the beam displacement fields. From a numerical point of view, linear equations are applied on the assembled finite element model. All slave nodes are eliminated, resulting in a reduction of the model size. Two examples have been presented: a straight beam and a curved beam with a square cross-section under distributed loading. Displacements and von Mises stresses have been observed for thin and thick cases. The FOSB model suffers from the Poisson thickness locking phenomenon, leading to wrong results. The MFOSB model is satisfactory for thin cases and leads to moderate errors for thick beams. The HOSB model gives excellent results in both the thin and thick cases, compared with the reference solid approach. These results show that the higher-order beam theory leads to a significant gain compared with the first-order beam theory for thick beams. This new solid-beam approach is efficient from the model size point of view. For the MFOSB model, the model size is comparable with that induced by using beam elements. For the HOSB model, the model size is intermediate between the beam and the solid models.

Many perspectives of development and applications of this solid-beam approach are possible. The extension to 3D beam and different types of cross-sections, leading to the treatment of more complex examples, is currently in progress. In particular warping namely due to torsion is a complex mechanical phenomenon as highlighted by numerous research works. From this point

of view, we are quite confident in the ability of our approach to take into account all possible and complex coupling effects highlighted in literature. Besides the solid elements considered in this paper, other solid finite elements with good performance could be exploited. This solid-beam approach can be extended to multilayered composite beam structures. An extension of the methodology is possible in the context of an adaptive approach in which different theories may be required depending on the area concerned. Indeed, several beam, shell, as well as the 3D theory of elasticity, can be taken into account in the same finite element model. The extension to nonlinear problem will be considered. Finally, the application to natural and industrial structures is a quite promising perspective.

Acknowledgements

The financial support from China Scholarship Council (CSC) and Université de Technologie de Compiègne (UTC) is gratefully acknowledged.

Appendix A. The coefficients for each cross-section of the MFOSB model

$$
\begin{cases}
a_1 = \dfrac{u_A - u_B}{z_A - z_B} \\[2ex]
a_2 = -\dfrac{z_A u_B - z_B u_A}{z_A - z_B} \\[2ex]
b_1 = \dfrac{v_D y_E - v_E y_D}{y_D y_E (z_D - z_E)} \\[2ex]
b_2 = \dfrac{v_E y_D z_D - v_D y_E z_E}{y_D y_E (z_D - z_E)} \\[2ex]
c_1 = -\dfrac{\begin{pmatrix} w_A y_B^2 z_C - w_A y_C^2 z_B - w_B y_A^2 z_C + w_B y_C^2 z_A + w_C y_A^2 z_B - w_C y_B^2 z_A - w_A y_B^2 z_D \\ +w_A y_D^2 z_B + w_A y_A^2 z_D - w_B y_D^2 z_A - w_D y_A^2 z_B + w_D y_B^2 z_A - w_C y_B^2 z_A - w_A y_B^2 z_D \\ +w_A y_C^2 z_D - w_A y_D^2 z_C - w_C y_A^2 z_D + w_C y_D^2 z_A + w_D y_A^2 z_C - w_D y_C^2 z_A - w_B y_C^2 z_D \\ +w_B y_D^2 z_C + w_C y_B^2 z_D - w_C y_D^2 z_B - w_D y_B^2 z_C + w_D y_C^2 z_B \end{pmatrix}}{\begin{pmatrix} -y_A^2 z_B^2 z_C + y_A^2 z_B^2 z_D + y_A^2 z_C^2 z_B - y_A^2 z_D^2 z_B - y_A^2 z_C^2 z_D + y_A^2 z_D^2 z_C + y_B^2 z_A^2 z_C - y_B^2 z_A^2 z_D \\ -y_B^2 z_C^2 z_A + y_B^2 z_D^2 z_A + y_B^2 z_C^2 z_D - y_B^2 z_D^2 z_C - y_C^2 z_A^2 z_B + y_C^2 z_A^2 z_D + y_C^2 z_B^2 z_A - y_C^2 z_D^2 z_A \\ -y_C^2 z_B^2 z_D + y_C^2 z_D^2 z_B + y_D^2 z_A^2 z_B - y_D^2 z_A^2 z_C - y_D^2 z_B^2 z_A + y_D^2 z_C^2 z_A + y_D^2 z_B^2 z_C \mp y_D^2 z_C^2 z_B \end{pmatrix}} \\[2ex]
c_4 = -\dfrac{\begin{pmatrix} w_A z_B z_C^2 - w_A z_C z_B^2 - w_B z_A z_C^2 + w_B z_C z_A^2 + w_C z_A z_B^2 - w_C z_B z_A^2 - w_A z_B z_D^2 + w_A z_D z_B^2 \\ +w_B z_A z_D^2 - w_B z_D z_A^2 - w_D z_A z_B^2 + w_B z_B z_A^2 + w_A z_C z_D^2 - w_A z_D z_C^2 - w_C z_A z_D^2 + w_C z_D z_A^2 \\ +w_D z_A z_C^2 - w_D z_C z_A^2 - w_B z_C z_D^2 + w_B z_D z_C^2 + w_C z_B z_D^2 - w_C z_D z_B^2 - w_D z_B z_C^2 + w_D z_C z_B^2 \end{pmatrix}}{\begin{pmatrix} -y_A^2 z_B^2 z_C + y_A^2 z_B^2 z_D + y_A^2 z_C^2 z_B - y_A^2 z_D^2 z_B - y_A^2 z_C^2 z_D + y_A^2 z_D^2 z_C + y_B^2 z_A^2 z_C - y_B^2 z_A^2 z_D \\ -y_B^2 z_C^2 z_A + y_B^2 z_D^2 z_A + y_B^2 z_C^2 z_D - y_B^2 z_D^2 z_C - y_C^2 z_A^2 z_B + y_C^2 z_A^2 z_D + y_C^2 z_B^2 z_A - y_C^2 z_D^2 z_A \\ -y_C^2 z_B^2 z_D + y_C^2 z_D^2 z_B + y_D^2 z_A^2 z_B - y_D^2 z_A^2 z_C - y_D^2 z_B^2 z_A + y_D^2 z_C^2 z_A + y_D^2 z_B^2 z_C \mp y_D^2 z_C^2 z_B \end{pmatrix}} \\[2ex]
c_2 = \dfrac{\begin{pmatrix} w_A y_B^2 z_C^2 - w_A y_C^2 z_B^2 - w_A y_A^2 z_C^2 + w_B y_C^2 z_A^2 + w_C y_A^2 z_B^2 - w_C y_B^2 z_A^2 - w_A y_B^2 z_D^2 + w_A y_D^2 z_B^2 \\ +w_B y_A^2 z_D^2 - w_B y_D^2 z_A^2 - w_D y_A^2 z_B^2 + w_D y_B^2 z_A^2 + w_A y_C^2 z_D^2 - w_A y_D^2 z_C^2 - w_C y_A^2 z_D^2 + w_C y_D^2 z_A^2 \\ +w_D y_A^2 z_C^2 - w_D y_C^2 z_A^2 - w_B y_C^2 z_D^2 + w_B y_D^2 z_C^2 + w_C y_B^2 z_D^2 - w_C y_D^2 z_B^2 - w_D y_B^2 z_C^2 + w_D y_C^2 z_B^2 \end{pmatrix}}{\begin{pmatrix} -y_A^2 z_B^2 z_C + y_A^2 z_B^2 z_D + y_A^2 z_C^2 z_B - y_A^2 z_D^2 z_B - y_A^2 z_C^2 z_D + y_A^2 z_D^2 z_C + y_B^2 z_A^2 z_C - y_B^2 z_A^2 z_D \\ -y_B^2 z_C^2 z_A + y_B^2 z_D^2 z_A + y_B^2 z_C^2 z_D - y_B^2 z_D^2 z_C - y_C^2 z_A^2 z_B + y_C^2 z_A^2 z_D + y_C^2 z_B^2 z_A - y_C^2 z_D^2 z_A \\ -y_C^2 z_B^2 z_D + y_C^2 z_D^2 z_B + y_D^2 z_A^2 z_B - y_D^2 z_A^2 z_C - y_D^2 z_B^2 z_A + y_D^2 z_C^2 z_A + y_D^2 z_B^2 z_C \mp y_D^2 z_C^2 z_B \end{pmatrix}} \\[2ex]
c_3 = \dfrac{\begin{pmatrix} w_D y_A^2 z_B^2 z_C - w_C y_A^2 z_B^2 z_D - w_D y_A^2 z_C^2 z_B + w_C y_A^2 z_D^2 z_B + w_B y_A^2 z_C^2 z_D - w_B y_A^2 z_D^2 z_C \\ -w_D y_B^2 z_A^2 z_C + w_C y_B^2 z_A^2 z_D + w_D y_D^2 z_C^2 z_A - w_C y_B^2 z_D^2 z_A - w_A y_B^2 z_C^2 z_D + w_A y_B^2 z_D^2 z_C \\ +w_D y_C^2 z_A^2 z_B - w_B y_C^2 z_A^2 z_D - w_D y_C^2 z_B^2 z_A + w_B y_C^2 z_D^2 z_A + w_A y_C^2 z_B^2 z_D - w_A y_C^2 z_D^2 z_B \\ -w_C y_D^2 z_A^2 z_B + w_B y_D^2 z_A^2 z_C + w_C y_D^2 z_B^2 z_A - w_B y_D^2 z_C^2 z_A - w_A y_D^2 z_B^2 z_C + w_A y_D^2 z_C^2 z_B \end{pmatrix}}{\begin{pmatrix} -y_A^2 z_B^2 z_C + y_A^2 z_B^2 z_D + y_A^2 z_C^2 z_B - y_A^2 z_D^2 z_B - y_A^2 z_C^2 z_D + y_A^2 z_D^2 z_C + y_B^2 z_A^2 z_C - y_B^2 z_A^2 z_D \\ -y_B^2 z_C^2 z_A + y_B^2 z_D^2 z_A + y_B^2 z_C^2 z_D - y_B^2 z_D^2 z_C - y_C^2 z_A^2 z_B + y_C^2 z_A^2 z_D + y_C^2 z_B^2 z_A - y_C^2 z_D^2 z_A \\ -y_C^2 z_B^2 z_D + y_C^2 z_D^2 z_B + y_D^2 z_A^2 z_B - y_D^2 z_A^2 z_C - y_D^2 z_B^2 z_A + y_D^2 z_C^2 z_A + y_D^2 z_B^2 z_C - +y_D^2 z_C^2 z_B \end{pmatrix}}
\end{cases}
$$

Reference

[1] S. P. Timoshenko, On the corrections for shear of the differential equation for transverse vibrations of prismatic bars, Philos. Mag. 41 (1921) 744–746.

[2] S. P. Timoshenko, On the transverse vibrations of bars of uniform cross section, Philos. Mag. 43 (1922) 125–131.

[3] G. R. Cowper, The shear coefficient in Timoshenko's beam theory, J. Appl. Mech. 33 (2) (1966) 335–340.

[4] J. J. Jensen, On the shear coefficient in Timoshenko's beam theory, J. Sound Vib. 87 (4) (1983) 621–635.

[5] J. R. Hutchinson, Shear coefficients for Timoshenko beam theory, J. Appl. Mech. 68 (1) (2001) 87–92.

[6] F. Essenburg, On the significance of the inclusion of the effect of transverse normal strain in problems involving beams with surface constraints, J. Appl. Mech. 42 (1) (1975) 127–132.

[7] N. G. Stephen, M. Levinson, A second order beam theory, J. Sound Vib. 67 (3) (1979) 293–305.

[8] M. Levinson, A new rectangular beam theory, J. Sound Vib. 74 (1) (1981) 81–87.

[9] L. W. Rehfield, P. L. N. Murthy, Toward a new engineering theory of bending: Fundamentals, AIAA J. 20 (5) (1982) 693–699.

[10] A. B. de Saint-Venant, Mémoire sur la torsion des prismes, Mémoires Des Savants Etrangers, 14 (1855) 233–560.

[11] V. Z. Vlasov, Thin walled elastic beams. Israel Program for Scientific Translations, Jerusalem, 1961.

[12] S. U. Benscoter, A theory of torsion bending for multicell beams, J. appl. Mech. 21 (1954) 25–34.

[13] R. Schardt, Generalized beam theory – an adequate method for coupled stability problems, Thin-Walled Struct. 19 (2–4) (1994) 161–180.

[14] A. K. Habtemariam, C. Könke, V. Zabel, M. J. Bianco, Generalized Beam Theory formulation for thin-walled pipes with circular axis, Thin-Walled Struct. 159 (2021) 107243.

[15] R. El Fatmi, A refined 1D beam theory built on 3D Saint-Venant's solution to compute homogeneous and composite beams, J. Mech. Mater. Struct. 11 (4) (2016) 345–378.

[16] F. Naccache, R. El Fatmi, Numerical free vibration analysis of homogeneous or composite beam using a refined beam theory built on Saint Venant's solution, Comput. Struct. 210 (2018) 102–121.

[17] P. Ladevèze, J. Simmonds, New concepts for linear beam theory with arbitrary geometry and loading, Eur. J. Mech. A Solids 17 (3) (1998) 377–402.

[18] G. Romano, A. Barretta, R. Barretta, On torsion and shear of Saint-Venant beams, Eur. J. Mech. A Solids 35 (2012) 47–60.

[19] S. A. Faghidian, Unified formulation of the stress field of Saint-Venant's flexure problem for symmetric cross-sections, Int. J. Mech. Sci. 111–112 (2016) 65–72.

[20] J. N. Goodier, S.P. Timoshenko, Theory of Elasticity, McGraw-Hill, NY, 1970.

[21] E. Carrera, G. Giunta, M. Petrolo, Beam structures, classical and advanced theories, John Willey & Sons Inc., NY, 2011.

[22] S. Cen, Y. Shang, Developments of Mindlin-Reissner plate elements, Math. Probl. Eng. 2015 (2015) 1-12.

[23] R. Bouclier, T. Elguedj, A. Combescure, Locking free isogeometric formulations of curved thick beams, Comput. Methods Appl. Mech. Eng. 245–246 (2012) 144–162.

[24] C. Adam, S. Bouabdallah, M. Zarroug, H. Maitournam, Improved numerical integration for locking treatment in isogeometric structural elements, Part I: Beams, Comput. Methods Appl. Mech. Eng. 279 (2014) 1–28.

[25] D. Addessi, P. Di Re, G. Cimarello, Enriched beam finite element models with torsion and shear warping for the analysis of thin-walled structures, Thin-Walled Struct. 159 (2021) 107259.

[26] J. Wackerfuß, F. Gruttmann, A mixed hybrid finite beam element with an interface to arbitrary three-dimensional material models, Comput. Methods Appl. Mech. Eng. 198 (27–29) (2009) 2053–2066.

[27] J. Wackerfuß, F. Gruttmann, A nonlinear hu-washizu variational formulation and related finite-element implementation for spatial beams with arbitrary moderate thick cross-sections, Comput. Methods Appl. Mech. Eng. 200 (17–20) (2011) 1671–1690.

[28] M. Lezgy-Nazargah, P. Vidal, O. Polit, A quasi-3D finite element model for the analysis of thin-walled beams under axial–flexural–torsional loads, Thin-Walled Struct. 164 (2021) 107811.

[29] S.W. Lee, Y. H. Kim, A new approach to the finite element modelling of beams with warping effect, Int. J. Numer. Methods Eng. 24 (12) (1987) 2327–2341.

[30] M. Zivkovic, M. Kojic, R. Slavkovic, N. Grujovic, A general beam finite element with deformable cross-section, Comput. Methods Appl. Mech. Eng. 190 (20–21) (2001), 2651–2680.

[31] J. L. Curiel Sosa, A. J. Gil, Analysis of a continuum-based beam element in the framework of explicit-FEM, Finite Elem. Anal. Des. 45 (8-9) (2009) 583–591.

[32] T. Belytschko, W. K. Liu, B. Moran, Nonlinear finite elements for continua and structures, John Wiley & Sons, Ltd, Chichester, 2000.

[33] K. Yoon, Y. Lee, P. S. Lee, A continuum mechanics based 3-D beam finite element with warping displacements and its modeling capabilities, Struct. Eng. Mech. 43 (4) (2012) 411–437.

[34] K. Yoon, P. S. Lee, Nonlinear performance of continuum mechanics based beam elements focusing on large twisting behaviors, Comput. Methods Appl. Mech. Eng. 281 (2014) 106–130.

[35] M. Ziyaeifar, H. Noguchi, A refined model for beam elements and beam-column joints, Comput. Struct. 76 (4) (2000) 551–564.

[36] J. Frischkorn, S. Reese, A solid-beam finite element and non-linear constitutive modelling, Comput. Methods Appl. Mech. Eng. 265 (2013) 195–212.

[37] M. Schwarze, S. Reese, A reduced integration solid-shell finite element based on the EAS and the ANS concept–large deformation problems, Int. J. Numer. Methods Eng. 85 (3) (2011) 289–329.

[38] J. Frischkorn, S. Reese, Solid-beam finite element analysis of nitinol stents, Comput. Methods Appl. Mech. Eng. 291 (2015) 42–63.

[39] Abaqus Analysis User's Guide, Abaqus 6.14, Dassault Systèmes Simulia, 2014.